NASA TECHNICAL NOTE

NASA TN D-2417

NASA TN D-2417

HEAT-TRANSFER MEASUREMENTS AT A MACH NUMBER OF 8 IN THE VICINITY OF A 90° INTERIOR CORNER ALINED WITH THE FREE-STREAM VELOCITY

by P. Calvin Stainback

Langley Research Center
Langley Station, Hampton, Va.

NATIONAL AERONAUTICS AND SPACE ADMINISTRATION • WASHINGTON, D. C. • AUGUST 1964

HEAT-TRANSFER MEASUREMENTS AT A MACH NUMBER OF 8 IN THE VICINITY OF A 90° INTERIOR CORNER ALINED WITH THE FREE-STREAM VELOCITY

By P. Calvin Stainback

Langley Research Center
Langley Station, Hampton, Va.

NATIONAL AERONAUTICS AND SPACE ADMINISTRATION

For sale by the Office of Technical Services, Department of Commerce,
Washington, D.C. 20230 -- Price $1.00

HEAT-TRANSFER MEASUREMENTS AT A MACH NUMBER OF 8 IN THE VICINITY OF A 90° INTERIOR CORNER ALINED WITH THE FREE-STREAM VELOCITY

By P. Calvin Stainback
Langley Research Center

SUMMARY

An experimental investigation was conducted to determine the influence of the interaction of the flow field with the boundary layer on the heat transfer in the vicinity of an interior corner formed by the normal intersection of two planes when the line of intersection was alined with the free-stream velocity. The investigation was made at a nominal Mach number of 8, and the nominal unit Reynolds number per foot was varied from 0.23×10^6 to 10.07×10^6.

The results indicated that the peak heating rate in the vicinity of the corner could be about 1.5 times the undisturbed flat-plate value outside the mutual boundary-layer interaction region. This high heating rate was attributed to the mutual interaction of the inviscid flow field with the boundary layer. Within the mutual boundary-layer interaction region a decrease in the heating rate was observed, and this result was in qualitative agreement with theoretical results.

INTRODUCTION

The flow of a fluid in the vicinity of an interior corner formed by two intersecting plates has received considerable theoretical and experimental attention in recent years since this simple geometric configuration can be expected to simulate adequately some of the major phenomena encountered on more complex junctions found in fluid machines, aircraft, and high-performance spacecraft.

Most of the theoretical investigations have been limited to the study of the boundary layer in the immediate vicinity of the corner. (See, for example, refs. 1 to 11.) This flow regime is designated herein as the near-corner viscous interaction region or simply the near-corner region. Until recently, most of the experimental investigations were limited to the study of the inviscid flow field and its ultimate interaction with the boundary layer outside the near-corner region (refs. 12 to 15). This region is designated herein as the far-corner interaction region. A theoretical study of the inviscid far-corner

interaction region can be found in reference 16 and an experimental study of the viscous near-corner region in reference 17. Recently, experimental studies conducted at a Mach number of 16 provided heat-transfer and pressure data in both the near and far interaction regions (refs. 18 and 19).

The present paper presents heat-transfer and flow-visualization data taken in both the near-corner and far-corner interaction regions at a Mach number of 8.00 and a range of Reynolds number per foot from 0.23×10^6 to 10.07×10^6. The present data are presented in somewhat more detail than the heat-transfer data of references 18 and 19 and because of the difference in the free-stream Mach number and should serve to supplement the data of these references.

SYMBOLS

$C = \frac{\delta}{x}\sqrt{R_x}$

$B = \left[N_{St}\sqrt{R_x}\right]_e \Big/ C$

h	aerodynamic heat-transfer coefficient, Btu/sec-ft^2-$^\circ$R
M_∞	free-stream Mach number
N_{St}	Stanton number based on free-stream conditions
p	pressure
q	aerodynamic heat-transfer rate, Btu/sec-ft^2
R	unit Reynolds number (per foot) based on free-stream conditions
R_x	Reynolds number based on free-stream conditions and distance from leading edge
T	temperature
x	distance from leading edge of model
y,z	coordinate distances from corner of model
δ	interaction boundary-layer thickness

Subscripts:

e	effective flat-plate value
t	stagnation conditions
w	wall condition

DESCRIPTION OF MODEL

The corner heat-transfer model was machined from a single piece of 17-4 PH stainless-steel bar stock. Its overall dimensions were 4.50 by 4.50 by 11 inches. (See fig. 1 for details.) The sides which formed the corner were 0.50 inch thick and these produced a corner with an inside dimension of 4.00 inches in the vertical and transverse directions. The model was instrumented from 0.050 inch to 2.00 inches from the corner and 0.50 inch to 9.75 inches from the leading edge. The leading-edge thickness was approximately 0.002 inch.

The thermocouple stations were formed by machining 0.50-inch transverse slots 2.50 inches long in the reverse side of the model to produce a skin thickness 0.015 inch. Near the leading edge, where the 0.50-inch slots would have overlapped, a large cavity was machined to receive the thermocouples. All cavities were shielded from the flow by the support system or by cover plates.

At the corner two milling operations, 90° apart, were made at each longitudinal station in order to form a corner with 0.015-inch-thick walls. (See fig. 1.) As a result of this method of machining, an excess mass 0.015 by 0.015 inch was formed opposite the line of intersection of the planes forming the corner. This mass received no direct aerodynamic heating from the model surface; the heat stored in this mass was received from adjacent metal by conduction. In an attempt to reduce this conduction, the inside corner of this mass was chamfered 0.015 inch by 45°. Thermocouples were located on the chamfered surface and were used to monitor the conduction effects of the excess mass on the thermocouples located 0.05 inch from the corner. The elementary analysis of reference 13 indicated that the effect of the excess mass on the heating rate determined by the thermocouples 0.05 inch from the corner was less than 4 percent. This possible error was not taken into account in reducing the present data.

A total of 80 iron-constantan thermocouples (0.010 inch in diameter) were installed in the model. The thermocouple junctions were made by spot welding individual thermocouple wires on the reverse side of the model skin. The coordinates of the thermocouple stations are given in the following table:

y, in.	x, in.									
0.05 .15 .35 .60 1.00 1.50 2.00	0.50	0.75	1.00	1.50	2.25	3.25	4.50	6.00	7.75	9.75

A second model was made similar to the heat-transfer model and was used for the temperature-sensitive-paint and oil-flow investigation. This model was covered with plastic and fiber glass, except in the vicinity of the leading edge, to provide an insulating surface desirable for use with the temperature-sensitive-paint investigation.

In order to obtain shadowgraphs of the shock inside the corner, a third model was constructed of steel; and a flat, front-surfaced mirror was set into the vertical side an inch from the leading edge. With this model it was possible to obtain double pass shadowgraphs of the shock generated by the transverse side of the model.

TEST PROCEDURE AND DATA REDUCTION

Testing of the corner model was conducted at the Langley Mach 8 variable-density tunnel. This tunnel is of the blowdown type and has an axially symmetric nozzle with contoured walls. The average test-section Mach number variation with stagnation pressure is presented in figure 2. The Mach numbers used to reduce the present data were obtained from an earlier partial calibration of the tunnel and except for the low stagnation pressure, where the earlier calibration curves were extrapolated, the results of the two calibrating curves were essentially the same.

The test-section unit Reynolds number per foot ranged from 0.23×10^6 to 10.07×10^6 for the heat-transfer tests; from 0.56×10^6 to 3.15×10^6 for the shadowgraph tests; and for the oil-flow and temperature-sensitive-paint investigation the Reynolds number per foot was 1.77×10^6.

The heat-transfer data were obtained by the transient-heating technique. This technique provided for the establishment of steady flow in the test section with the model outside the tunnel; after steady operation had been obtained the model was inserted into the test section. The model was removed from the test section after about 4 seconds and was brought to isothermal conditions at approximately room temperature. The transient-heating times required to move the model through the tunnel boundary layer was about 0.05 second, and care was taken to eliminate this effect on measured temperature during data reduction.

The heat-transfer data were obtained by recording the temperature-time history of the model on magnetic tape with a digital data recorder. The temperature data were reduced to heating rates and Stanton number on a digital computing machine. (See ref. 20 for the details of data reduction.)

The temperature-sensitive-paint, oil-flow, and shadowgraph tests were similar to the heat-transfer tests. The temperature-sensitive-paint model is shown mounted on the test-section injection mechanism in the retracted position in figure 3.

The temperature-sensitive paint has the characteristic that the paint changes color as its temperature is increased. The paint used was a four-color-change type; however, only one color change was experienced during the present tests. This color change occurred from pink, the original color, to blue. A more detailed description of this paint and testing technique can be found in reference 21.

DISCUSSION OF RESULTS

The heat-transfer data in the form of Stanton number are presented in figure 4 as a function of Reynolds number for various unit Reynolds numbers and distances from the corner. The data are presented in tabular form in table I. Theoretical low-speed laminar (ref. 22) and turbulent (ref. 23) flat-plate heating curves are included in the figure for comparison with the present data. For reference, the leading-edge boundary-layer induced shock location, obtained from the shadowgraph results presented in figure 5, is also included in the figure. In figure 5(a) the shock location is indicated by its reflection from the mirror which is set into the vertical side of the model. Also presented in figure 5(b) are plots of shock locations for various unit Reynolds numbers. Some of these curves were obtained by extrapolating the measured data. It should be noted that the Reynolds number based on the shock distance from the leading edge is outside the Reynolds number range shown in some of the plots in figure 4.

At $y = 2.00$ and 1.50 inches, the Stanton number (fig. 4) agrees quite well with the theoretical laminar values except for $R_x > 4 \times 10^6$ where the disagreement can be attributed to transitional or turbulent flow. Although the shock crosses the $y = 1.50$ location ahead of the last thermocouple, there is little if any indication of this disturbance on the heating rate except for the aforementioned transition which will be discussed subsequently. As y is decreased to 1.00 inch there is some indication of an increase in the Stanton number behind the shock. This phenomenon is most evident at the lower unit Reynolds numbers. A further decrease in y to 0.60 inch reveals a pronounced increase in heating behind the shock and this increase is evident as y is decreased to 0.05 inch. At $y = 0.05$ inch the Stanton number is substantially less than the theoretical laminar value for large values of x. This decrease can be attributed to the mutual interaction of the boundary layers in the vicinity of the corner, a result in agreement with the near-corner interaction theories.

The regions with heating rates higher than the undisturbed laminar values are located in the far interaction regions and result from the mutual interaction of the two inviscid flow fields associated with the two plates forming the corner and their ultimate interaction with the boundary layer. The maximum value of this increased heating is about 1.5 to 2.0 times the theoretical laminar value and occurs at about 0.35 inch from the corner.

The area where the increase in heating occurs is well downstream of the projected shock location. This result can be seen from figure 4 and also from figure 6. This latter figure presents the temperature-sensitive-paint results. The dark areas (blue) represent regions with higher heating rates than the light areas (pink). The shock position has been superimposed on the photograph

and the high heating region is located downstream of the shock. This condition is more evident at large distances from the leading edge as a result of the "conical like" disturbances which originate at the leading edge of the corner.

It is interesting to note from figure 4 that if data were available only over a limited Reynolds number range, the increase in heating might erroneously be attributed to transition. However, for sufficiently large values of the Reynolds number the heating rate downstream of the peak heating region tends to decrease toward the laminar value. In fact, a comparison of the transition data at $R_x = 10.07 \times 10^6$ (per foot) for decreasing values of y from 2.00 to 0.05 inch indicates that the corner flow which causes the increased heating tends to suppress transition.

There is a slight indication that the heating rate in the immediate vicinity of the shock is reduced below the undisturbed value. This phenomenon can be seen a little clearer when the parameter $N_{St}\sqrt{R_x}$ is plotted as a function of x. Such a plot is presented in figure 7 for $y = 1.50$ inches, 0.60 inch, and 0.35 inch. If the data for $y = 1.50$ inches are assumed to represent the undisturbed flow over the model and a curve is faired through the data for all values of y, then a slight reduction in the heating rate in the vicinity of the shock can be discerned. This result suggests the possibility that the shock tends to produce an incipient boundary-layer-separation condition with its attendant thickening of the boundary layer.

In reference 11 the reduction in the heating rate within the mutual boundary-layer interaction region was found to vary linearly with distance from the corner. This variation can be expressed as

$$\frac{q}{q_e} = \frac{y}{\delta} \qquad (0 \leq y \leq \delta) \qquad (1)$$

If the definition of the aerodynamic-heat-transfer coefficient is used and the wall is assumed to be isothermal, equation (1) can be expressed as follows:

$$\frac{h}{h_e} = \frac{y}{\delta} \qquad (0 \leq y \leq \delta) \qquad (2)$$

This equation can be given in terms of the Stanton number and Reynolds number, based on free-stream conditions, as

$$\frac{N_{St}\sqrt{R_x}}{\left[N_{St}\sqrt{R_x}\right]_e} = \frac{y}{\delta} \qquad (0 \leq y \leq \delta) \qquad (3)$$

The interaction boundary-layer thickness can be expressed as (ref. 1)

$$\frac{\delta}{x} = \frac{C}{\sqrt{R_x}} \qquad (4)$$

where C is a constant for a corner model with zero streamwise pressure gradient. Substituting equation (4) into (3) gives

$$N_{St}\sqrt{R_x} = B\,\frac{y}{x}\sqrt{R_x} \qquad (0 \leqq y \leqq \delta) \qquad (5)$$

where B is a constant and equal to $\left[N_{St}\sqrt{R_x}\right]_e \Big/ C$, provided the streamwise pressure gradient is negligible.

The heat-transfer data are presented in terms of the parameters of equation (5) for several free-stream unit Reynolds numbers in figure 8. This figure indicates that the variation of the heating rate with distance from the corner in the interaction region is essentially linear within the limits of the present investigation and tends to confirm the theoretical finding of reference 11.

For the present test conditions, the "undisturbed" conditions exterior to the near-corner viscous-interaction region are not the flat-plate values but would be the conditions between the near-corner region and the high heating region in the far-corner region.

From figure 8 this value of $\left[N_{St}\sqrt{R_x}\right]_e$ appears to be constant for all unit Reynolds numbers and has a value of about 0.475. Curves fitted to the data near the corner indicate that the value of B varies with unit Reynolds number and if $\left[N_{St}\sqrt{R_x}\right]_e$ is assumed constant, the value of C must vary with unit Reynolds number. This variation is shown in figure 9, where C is determined by the intersection of the faired curve with the assumed constant value of $\left[N_{St}\sqrt{R_x}\right]_e$ of 0.475. Values for C can also be obtained from figure 4 for $y = 0.05$ inch if it is assumed that the near-corner interaction region begins when the Stanton number deviates from the flat-plate-like variation that it has near the leading edge. Values for C calculated in this manner are also shown in figure 9 and the agreement in estimating C by the two methods is good. A curve fitted to the data indicated that $C \approx R^{0.459}$. The power of the unit Reynolds number is nearly 0.5 and indicates that δ is almost independent of unit Reynolds number and, therefore, is almost proportional to $\sqrt{x}$. Also, the heat-transfer parameter $N_{St}\sqrt{R_x}$ in the boundary-layer interaction region should correlate in terms of the geometric quantity $y/\sqrt{x}$. In figure 10 the heat-transfer parameter $N_{St}\sqrt{R_x}$ is plotted as a function of $y/\sqrt{x}$ and shows that in the near-corner region the heat-transfer parameter can be correlated reasonably well in terms of this geometric quantity.

That δ is almost independent of unit Reynolds number can be seen by calculating δ for $R = 0.23 \times 10^6$ and $R = 10.07 \times 10^6$ from the values of C obtained from the curve in figure 9. These calculations would reveal that δ changes only 16 percent, whereas if C were a constant, δ would vary by a factor of 6.6.

Attempts were made to determine the reason for the relative invariance of δ with unit Reynolds number. The variation of δ can be influenced by the

boundary-layer induced pressure on the plate, which would be more effective in thinning the boundary layer for low unit Reynolds number than for high values. Reference 11 indicated that for Mach numbers greater than about 3.5 the boundary layer in the corner is "square," that is, the interaction boundary layer is equal to the undisturbed value. From this result the undisturbed boundary-layer thickness was approximated by estimating the pressure distribution, the ratio of the boundary-layer thickness in a pressure gradient to the zero-pressure-gradient value, and the zero-pressure-gradient boundary-layer thickness from references 24, 25, and 26, respectively. The results of these calculations are shown in figure 9 as a crosshatched area since C varies with x for cases where a pressure gradient exists. (It should be noted that C for the present case probably varies with x for a given unit Reynolds number, but the data are not sufficiently detailed to reveal this variation.) From figure 9 it can be seen that for the lowest unit Reynolds numbers the measured values of C and also δ are about one-half the estimated undisturbed values. This result indicates that some other phenomenon must be responsible for reducing the extent of the interaction boundary layer.

It was postulated in reference 27 that the leading edge of the corner produced a vortex system in the vicinity of the corner. If this postulate were correct, the vortex could influence the extent of the near-corner region by altering the flow at the outer edge of the boundary layer. In order to investigate the existence of a vortex system in the vicinity of the corner, several oil-flow tests were conducted. These tests were performed both by coating the corner model completely with a mixture of oil and lamp black and by using discrete dots of the mixture. Results of the test at a unit Reynolds number per foot of 1.77×10^6 of the completely coated model is shown in figures 11(a) and 11(b); results of the discrete-dot method are shown in figure 11(c). The two photographs in figures 11(a) and 11(c) show the general flow pattern obtained from both test methods. The other (fig. 11(b)) shows a closeup of the flow pattern in the vicinity of the corner and leading edge.

The flow pattern obtained from the model completely coated with the oil-lamp-black mixture reveals a high shear region near the leading edge in the vicinity of the corner. This result is in general agreement with the temperature-sensitive-paint results presented in figure 6, that is, the high heating region revealed by the temperature-sensitive-paint results is due to the fact that the shear stresses in the boundary layer are higher in the region of high heat-transfer rate than in adjacent regions. This result could be indicative of a vortex system in the vicinity of the corner.

The oil-flow results indicate some outflow from the corner which is greater than the outflow that could be expected from displacement effects. This effect could also be indicative of a vortex system.

CONCLUSIONS

The experimental investigation, at a Mach number of 8, of the flow in the vicinity of the corner formed by two perpendicular plates alined with the free-stream velocity permits the following conclusions to be stated:

1. A high heat-transfer region exterior to the mutual boundary-layer-interaction region is associated with the flow-field interaction between the two plates and its ultimate interactions with the boundary layer. The heating in this region is approximately 1.5 theoretical flat-plate value without the flow-field interaction.

2. Within the mutual boundary-layer-interaction region a decrease occurs in the heating rate that is in qualitative agreement with rates from recent compressible-flow theory.

3. The mutual boundary-layer-interaction thickness as deduced from heat-transfer tests is relatively insensitive to the free-stream unit Reynolds number and is therefore almost proportional to $\sqrt{x}$, where x is the distance from the leading edge.

4. A slight reduction in the heating that takes place in the vicinity of the boundary-layer induced shock is apparently associated with a thickening of the boundary layer due to incipient boundary-layer-separation conditions caused by the shock.

Langley Research Center,
National Aeronautics and Space Administration,
Langley Station, Hampton, Va., May 13, 1964.

REFERENCES

1. Loiziansky, L. G.: Interference of Boundary Layers. No. 249, Trans. Central Aero-Hydrodynamical Inst. (Moscow), 1936.

2. Loitsianskii, L. G., and Bolshakov, V. P.: On Motion of Fluid in Boundary Layer Near Line of Intersection of Two Planes. NACA TM 1308, 1951.

3. Carrier, G. F.: The Boundary Layer in a Corner. Quarterly Appl. Math., vol. IV, no. 4, Jan. 1947, pp. 367-370.

4. Sowerby, L., and Cooke, J. C.: The Flow of Fluid Along Corners and Edges. Quarterly Jour. Mech. and Appl. Math., vol. VI, pt. 1, Mar. 1953, pp. 50-70.

5. Dowdell, Rodger Birtwell: Corner Boundary Layer. M.S. Thesis, Yale Univ., 1952.

6. Oman, Richard A.: The Three-Dimensional Laminar Boundary Layer Along a Corner. Tech. Rep. No. 1 (Contract No. DA-19-020-ORD-4538), M.I.T., Jan. 1959. (Available from ASTIA as AD 211216.)

7. Kemp, Nelson Harvey: The Laminar Three-Dimensional Boundary Layer and a Study of the Flow Past a Side Edge. M. Aero. Eng. Thesis, Cornell Univ., June 1951. (Available from ASTIA as AD 45462.)

8. Levy, Richard H.: The Boundary Layer in a Corner. Contract AF 49(638)-465, Dept. Aero. Eng., Princeton Univ., Nov. 1959.

9. Cheng, Sin-I, and Levy, Richard H.: The Boundary Layer in a Corner. Rep. No. 485 (AFOSR TN 59-1165), Princeton Univ., Nov. 1959.

10. Krzywoblocki, M. Z.: On the Boundary Layer in a Corner by Use of the Relaxation Method. Ganita (Lucknow, India), vol. 7, no. 2, Dec. 1956, pp. 76-112.

11. Bloom, Martin H., and Rubin, Stanley: High-Speed Viscous Corner Flow. Jour. Aerospace Sci., vol. 28, no. 2, Feb. 1961, pp. 145-157.

12. Galowin, Lawrence: Heat Transfer Correlations for 90° Corner Interference Effects on Fin-Flat Plate Model at a Mach Number of 8. Tech. Rep. No. 207 (Contract No. AF 33(616)-6692), Gen. Appl. Sci. Labs., Inc., Feb. 8, 1961.

13. Stainback, P. Calvin: An Experimental Investigation at a Mach Number of 4.95 of Flow in the Vicinity of a 90° Interior Corner Alined With the Free-Stream Velocity. NASA TN D-184, 1960.

14. Rhudy, J. P., Hiers, R. S., and Rippey, J. O.: Pressure Distribution and Heat Transfer Test on Two Fin-Flat Plate Interference Models and Several Blunt Leading Edge Delta Wing Models. AEDC-TN-60-168 (Contract No. AF 40(600)-800S/A 11(60-110)), Arnold Eng. Dev. Co., Sept. 1960.

15. Jones, Robert A.: Heat-Transfer and Pressure Investigation of a Fin-Plate Interference Model at a Mach Number of 6. NASA TN D-2028, 1964.

16. Hains, Franklin D.: Supersonic Flow Near the Junction of Two Wedges. Jour. Aero/Space Sci. (Readers' Forum), vol. 25, no. 8, Aug. 1958, pp. 530-531.

17. Gersten, K.: Corner Interference Effects. NATO Rep. 299, AGARD, North Atlantic Treaty Organization (Paris), Mar. 1959.

18. Miller, D. S., Hijman, R., Redeker, E., Janssen, W. C., and Mullen, C. R.: A Study of Shock Impingements on Boundary Layers at Mach 16. Proc. 1962 Heat Transfer and Fluid Mechanics Inst. (Univ. Wash.), F. Edward Ehlers, James J. Kauzlarich, Charles A. Sleicher, Jr., and Robert E. Street, eds., Stanford Univ. Press, June 1962, pp. 255-278.

19. Caldwell, A. L., Haugseth, E. G., and Miller, D. S.: The Influence of Aerodynamic Interference Heating on Directional Stability Problems of Hypersonic Vehicles. Paper 63-6, Inst. Aerospace Sci., Jan. 1963.

20. Stainback, P. Calvin: Heat-Transfer Measurements at a Mach Number of 4.95 on Two 60° Swept Delta Wings With Blunt Leading Edges and Dihedral Angles of 0° and 45°. NASA TN D-549, 1961.

21. Stainback, P. Calvin: A Visual Technique for Determining Qualitative Aerodynamic Heating Rates on Complex Configurations. NASA TN D-385, 1960.

22. Eckert, Ernst R. G.: Survey on Heat Transfer at High Speeds. WADC Tech. Rep. 54-70, U.S. Air Force, Apr. 1954.

23. Van Driest, E. R.: The Problem of Aerodynamic Heating. Aero. Eng. Rev., vol. 15, no. 10, Oct. 1956, pp. 26-41.

24. Bertram, Mitchel H.: Boundary-Layer Displacement Effects in Air at Mach Numbers of 6.8 and 9.6. NASA TR R-22, 1959. (Supersedes NACA TN 4133.)

25. Bertram, Mitchel H., and Feller, William V.: A Simple Method for Determining Heat Transfer, Skin Friction, and Boundary-Layer Thickness for Hypersonic Laminar Boundary-Layer Flows in a Pressure Gradient. NASA MEMO 5-24-59L, 1959.

26. Van Driest, E. R.: Investigation of Laminar Boundary Layer in Compressible Fluids Using the Crocco Method. NACA TN 2597, 1952.

27. Bogdonoff, S. M., and Vas, I. E.: A Preliminary Investigation of the Flow in a 90° Corner at Hypersonic Speeds. Part I - Flat Plates With Thin Leading Edges at Zero Angle of Attack. D-143-978-013 (ARDC TR 57-202, AD 150 023), Bell Aircraft Corp., Dec. 20, 1957.

TABLE I.- HEAT-TRANSFER DATA

(a) $R = 0.23 \times 10^6$; $T_t = 1105^\circ$ R; $p_t = 36.6$ psia; $M_\infty = 7.72$

x, in.	q, Btu/sec-ft^2	T_w, $^\circ$F	h, Btu/sec-ft^2-$^\circ$F
y = 0.05 in.			
0.50	0.26063	78.03	0.00059
.75	.21610	77.37	.00049
1.00	.16720	75.97	.00038
1.50	.14209	75.97	.00032
2.25	.07739	74.81	.00017
3.25	.06237	74.91	.00014
4.50	-------	-----	-------
6.00	.02822	74.52	.00006
7.75	.02109	74.51	.00005
9.75	.01610	73.67	.00004
y = 0.15 in.			
0.50	0.26145	77.95	0.00059
.75	.20379	76.07	.00046
1.00	.18100	75.94	.00041
1.50	.16122	75.75	.00036
2.25	.12897	75.39	.00029
3.25	.08811	76.24	.00020
4.50	.05310	74.42	.00012
6.00	.06102	74.93	.00014
7.75	.06248	74.82	.00014
9.75	.02458	74.65	.00006
y = 0.35 in.			
0.50	0.24719	77.70	0.00056
.75	-------	-----	-------
1.00	.14770	75.39	.00033
1.50	.14402	75.14	.00032
2.25	.13430	76.19	.00030
3.25	.14694	75.28	.00033
4.50	.12452	75.06	.00028
6.00	.10126	75.28	.00022
7.75	.08632	75.25	.00019
9.75	.06097	75.21	.00014
y = 0.60 in.			
0.50	0.27347	76.65	0.00062
.75	.20382	75.90	.00046
1.00	.16001	76.64	.00036
1.50	.13992	75.20	.00031
2.25	.11761	75.75	.00030
3.25	.08499	75.55	.00019
4.50	.09469	76.00	.00022
6.00	.09951	75.45	.00022
7.75	.09968	74.98	.00022
9.75	.10528	74.79	.00023
y = 1.00 in.			
0.50	0.25799	77.83	0.00058
.75	.18498	75.99	.00042
1.00	.14842	76.57	.00033
1.50	.12642	75.21	.00028
2.25	.09445	76.02	.00021
3.25	.07797	75.39	.00018
4.50	.05780	74.64	.00013
6.00	.06430	75.08	.00014
7.75	.06896	75.71	.00015
9.75	.06164	75.31	.00001
y = 1.50 in.			
0.50	0.25564	76.07	0.00058
.75	.20065	75.47	.00045
1.00	.15915	75.30	.00036
1.50	.15420	74.96	.00034
2.25	.10557	74.72	.00023
3.25	.07555	75.09	.00017
4.50	.06094	74.69	.00014
6.00	.05295	74.86	.00012
7.75	.05515	74.72	.00012
9.75	.05006	74.64	.00011
y = 2.00 in.			
0.50	0.25476	78.25	0.00058
.75	.18046	77.33	.00041
1.00	.16406	77.14	.00037
1.50	.13503	75.30	.00030
2.25	.10346	74.92	.00023
3.25	.08289	74.81	.00019
4.50	.06316	75.38	.00014
6.00	.06029	74.73	.00014
7.75	.05413	75.03	.00012
9.75	.05300	74.79	.00012

(b) $R = 0.42 \times 10^6$; $T_t = 1200^\circ$ R; $p_t = 73.2$ psia; $M_\infty = 7.74$

x, in.	q, Btu/sec-ft^2	T_w, $^\circ$F	h, Btu/sec-ft^2-$^\circ$F
y = 0.05 in.			
0.50	0.44911	78.67	0.00085
.75	.35987	80.08	.00068
1.00	.29034	79.28	.00055
1.50	.23508	77.88	.00045
2.25	.14943	76.20	.00029
3.25	.11037	75.12	.00021
4.50	-------	-----	-------
6.00	.05085	74.98	.00010
7.75	.03985	74.63	.00008
9.75	.36777	73.54	.00028
y = 0.15 in.			
0.50	0.45093	77.95	0.00086
.75	.36868	79.71	.00070
1.00	.31417	77.16	.00060
1.50	.27388	78.82	.00052
2.25	.22534	76.85	.00042
3.25	.18249	76.74	.00035
4.50	.09576	75.46	.00018
6.00	.10694	75.35	.00020
7.75	.07799	74.97	.00015
9.75	.07692	75.32	.00013
y = 0.35 in.			
0.50	0.43956	77.83	0.00083
.75	-------	-----	-------
1.00	.25323	76.43	.00048
1.50	.23762	77.43	.00045
2.25	.22603	76.09	.00042
3.25	.21759	76.00	.00041
4.50	.20315	77.32	.00038
6.00	.18766	77.17	.00032
7.75	.13878	75.96	.00026
9.75	.12240	75.17	.00023
y = 0.60 in.			
0.50	0.45138	78.42	0.00086
.75	.36107	79.38	.00069
1.00	.28200	78.32	.00053
1.50	.22271	77.25	.00042
2.25	.16561	75.34	.00031
3.25	.14618	74.93	.00028
4.50	.15917	76.52	.00030
6.00	.13710	76.87	.00032
7.75	.17137	74.95	.00032
9.75	.16249	75.10	.00031
y = 1.00 in.			
0.50	0.41207	77.99	0.00078
.75	.33251	79.27	.00063
1.00	.27406	76.61	.00052
1.50	.20671	77.29	.00039
2.25	.17686	76.91	.00034
3.25	.13442	75.64	.00025
4.50	.10654	75.13	.00020
6.00	.10217	74.61	.00018
7.75	.11419	75.67	.00022
9.75	.09945	74.96	.00019
y = 1.50 in.			
0.50	0.42234	77.80	0.00080
.75	.33488	76.82	.00063
1.00	.27941	76.38	.00053
1.50	.20362	76.79	.00038
2.25	.18393	75.03	.00035
3.25	.14434	75.20	.00027
4.50	.11270	75.05	.00021
6.00	.08984	74.40	.00017
7.75	.09649	74.69	.00018
9.75	.08765	75.13	.00017
y = 2.00 in.			
0.50	0.44479	78.37	0.00085
.75	.35454	77.33	.00067
1.00	.29029	77.08	.00055
1.50	.20770	77.81	.00039
2.25	.17947	74.94	.00034
3.25	.15138	75.13	.00029
4.50	.12017	74.83	.00023
6.00	.10064	74.04	.00019
7.75	.08795	74.36	.00017
9.75	.07858	75.02	.00015

(c) $R = 0.56 \times 10^6$; $T_t = 1285^\circ$ R; $p_t = 122$ psia; $M_\infty = 7.765$

x, in.	q, Btu/sec-ft^2	T_w, $^\circ$F	h, Btu/sec-ft^2-$^\circ$F
y = 0.05 in.			
0.50	0.64086	89.06	0.00109
.75	.54181	87.29	.00092
1.00	.45629	85.77	.00077
1.50	.36137	83.90	.00061
2.25	.20423	82.83	.00035
3.25	.14413	82.26	.00024
4.50	-------	-----	-------
6.00	.07022	83.32	.00012
7.75	.04412	83.44	.00007
9.75	.03602	82.97	.00006
y = 0.15 in.			
0.50	0.59579	89.61	0.00101
.75	.51599	87.81	.00087
1.00	.42425	89.25	.00072
1.50	.39649	88.49	.00067
2.25	.33427	85.13	.00056
3.25	.26902	84.78	.00046
4.50	.14297	85.59	.00024
6.00	.14994	85.11	.00026
7.75	.15182	84.83	.00026
9.75	.10382	85.85	.00018
y = 0.35 in.			
0.50	0.62005	90.01	0.00106
.75	.44326	88.08	.00075
1.00	.34627	86.63	.00059
1.50	.33887	85.10	.00057
2.25	.30401	85.19	.00051
3.25	.30177	87.47	.00051
4.50	.30495	86.17	.00051
6.00	.26586	88.57	.00045
7.75	.26863	86.91	.00045
9.75	.20635	87.96	.00035
y = 0.60 in.			
0.50	0.63261	91.56	0.00108
.75	.50099	89.54	.00085
1.00	.40584	89.89	.00069
1.50	.31966	85.39	.00054
2.25	.22179	84.77	.00037
3.25	.18411	84.67	.00031
4.50	.21520	85.63	.00036
6.00	.22681	86.74	.00038
7.75	.23147	87.36	.00039
9.75	.19778	89.76	.00034
y = 1.00 in.			
0.50	0.60323	91.93	0.00103
.75	.45616	89.76	.00078
1.00	.40965	88.15	.00069
1.50	.33968	88.61	.00058
2.25	.25272	85.93	.00042
3.25	.20050	86.76	.00034
4.50	.16310	87.34	.00027
6.00	.14234	87.52	.00024
7.75	.15722	88.57	.00027
9.75	.16828	89.59	.00028
y = 1.50 in.			
0.50	0.60534	92.28	0.00103
.75	.47459	93.19	.00081
1.00	.41340	88.43	.00070
1.50	.31799	87.18	.00054
2.25	.26288	88.55	.00044
3.25	.22308	87.95	.00037
4.50	.15250	86.99	.00026
6.00	.13071	88.59	.00022
7.75	.10939	88.71	.00019
9.75	.11633	90.26	.00019
y = 2.00 in.			
0.50	0.57875	97.48	0.00099
.75	.47811	94.96	.00082
1.00	.40304	93.32	.00069
1.50	.31024	91.19	.00053
2.25	.26741	89.18	.00046
3.25	.21939	88.57	.00037
4.50	.17804	87.63	.00030
6.00	.13790	89.80	.00023
7.75	.12439	89.73	.00021
9.75	.12321	90.08	.00021

(d) $R = 0.96 \times 10^6$; $T_t = 1320^\circ$ R; $p_t = 211$ psia; $M_\infty = 7.81$

x, in.	q, Btu/sec-ft^2	T_w, $^\circ$F	h, Btu/sec-ft^2-$^\circ$F
y = 0.05 in.			
0.50	0.89662	88.19	0.00146
.75	.71146	86.77	.00115
1.00	.56021	85.42	.00091
1.50	.44630	84.10	.00072
2.25	.15408	83.57	.00043
3.25	.16600	83.00	.00027
4.50	.01158	73.28	.00002
6.00	.07297	82.76	.00012
7.75	.01388	83.30	.00002
9.75	.01350	82.75	.00002
y = 0.15 in.			
0.50	0.76446	88.89	0.00124
.75	.62074	87.49	.00101
1.00	.54628	86.35	.00089
1.50	.61971	85.80	.00100
2.25	.47143	85.48	.00076
3.25	.09272	85.31	.00061
4.50	.56733	86.28	.00092
6.00	.20079	83.83	.00033
7.75	.17441	84.88	.00028
9.75	.11276	85.86	.00187
y = 0.35 in.			
0.50	0.73740	89.62	0.00120
.75	.51874	88.13	.00084
1.00	.46248	86.94	.00075
1.50	.39597	85.68	.00064
2.25	.37127	85.86	.00060
3.25	.38912	85.98	.00071
4.50	.37681	86.09	.00061
6.00	.36806	86.21	.00060
7.75	.33656	86.77	.00055
9.75	.27649	87.91	.00045
y = 0.60 in.			
0.50	0.77748	91.19	0.00127
.75	.60935	89.67	.00099
1.00	.47864	87.93	.00078
1.50	.39685	86.17	.00064
2.25	.30247	85.97	.00049
3.25	.33988	85.68	.00039
4.50	.26072	85.95	.00042
6.00	.28730	86.80	.00046
7.75	.27761	87.26	.00045
9.75	.26705	88.34	.00044
y = 1.00 in.			
0.50	0.73763	91.82	0.00121
.75	.57505	89.98	.00094
1.00	.49932	88.76	.00081
1.50	.02166	86.20	.00004
2.25	.31941	87.32	.00052
3.25	.26219	86.84	.00043
4.50	.21387	87.04	.00034
6.00	.01454	86.12	.00002
7.75	.01437	87.21	.00002
9.75	.17338	88.82	.00028
y = 1.50 in.			
0.50	0.75748	92.15	0.00124
.75	.61134	90.69	.00100
1.00	.50156	89.16	.00082
1.50	.44052	88.35	.00071
2.25	.32252	88.12	.00053
3.25	.27247	87.88	.00044
4.50	.21578	87.92	.00035
6.00	.19222	88.13	.00031
7.75	.16917	88.27	.00028
9.75	.13265	89.85	.00022
y = 2.00 in.			
0.50	0.77322	92.38	0.00126
.75	.61822	91.23	.00101
1.00	.53411	90.45	.00087
1.50	.43914	89.52	.00071
2.25	.34565	88.55	.00056
3.25	.28786	88.23	.00047
4.50	.02800	87.38	.00004
6.00	.18307	89.04	.00030
7.75	.16779	89.28	.00027
9.75	.13260	90.46	.00022

TABLE I.- HEAT-TRANSFER DATA - Concluded

(e) $R = 1.77 \times 10^6$; $T_t = 1358^\circ$ R; $p_t = 395$ psia; $M_\infty = 7.87$

x, in.	q, Btu/sec-ft^2	T_w, $^\circ$F	h, Btu/sec-ft^2-$^\circ$F
	y = 0.05 in.		
0.50	1.18067	96.18	0.00184
.75	.92570	99.14	.00145
1.00	.79925	91.62	.00124
1.50	.66764	89.64	.00103
2.25	.42450	90.85	.00066
3.25	.32436	88.37	.00495
4.50	-------	------	-------
6.00	.16529	86.38	.00256
7.75	.13060	86.37	.00020
9.75	.06981	84.85	.00010
	y = 0.15 in.		
0.50	1.11039	95.08	0.00173
.75	.86229	92.64	.00133
1.00	.76050	91.19	.00117
1.50	.77347	91.24	.00119
2.25	.59261	90.43	.00918
3.25	.45180	92.40	.00070
4.50	.28290	89.85	.00432
6.00	.28727	87.35	.00440
7.75	.25451	87.72	.00039
9.75	.19271	89.78	.00299
	y = 0.35 in.		
0.50	1.06218	95.72	0.00165
.75	.76616	92.77	.00119
1.00	.63644	91.14	.00098
1.50	.57922	89.71	.00089
2.25	.51449	90.13	.00797
3.25	.50652	93.39	.00784
4.50	.43431	93.96	.00720
6.00	.46441	89.96	.00720
7.75	.41630	92.24	.00064
9.75	.33050	92.80	.00513
	y = 0.60 in.		
0.50	1.13061	104.40	0.00178
.75	.92766	100.28	.00145
1.00	.68331	96.73	.00106
1.50	.58871	90.39	.00091
2.25	.42917	92.54	.00067
3.25	.34972	90.94	.00054
4.50	.35149	92.11	.00054
6.00	.38130	92.90	.00059
7.75	.39842	92.20	.00062
9.75	.34662	90.86	.00053
	y = 1.00 in.		
0.50	1.05975	104.28	0.00167
.75	.82727	100.24	.00129
1.00	.69375	93.38	.00108
1.50	.59662	91.93	.00092
2.25	.45993	91.25	.00071
3.25	.33137	92.26	.00051
4.50	.27781	89.86	.00043
6.00	.25982	91.29	.00040
7.75	.26815	89.97	.00041
9.75	.27033	92.66	.00040
	y = 1.50 in.		
0.50	1.04059	98.20	0.00016
.75	.87012	95.96	.00136
1.00	.72503	93.91	.00113
1.50	.53253	95.86	.00083
2.25	.46540	92.34	.00072
3.25	.39026	91.29	.00061
4.50	.30356	91.01	.00047
6.00	.25190	92.71	.00039
7.75	.23033	91.60	.00036
9.75	.20916	91.72	.00033
	y = 2.00 in.		
0.50	1.08857	100.57	0.00170
.75	.88174	98.28	.00138
1.00	.75516	96.83	.00118
1.50	.60542	95.20	.00094
2.25	.49020	96.18	.00077
3.25	.44313	91.71	.00069
4.50	.31252	93.76	.00049
6.00	.27471	91.64	.00042
7.75	.24804	91.33	.00038
9.75	.22102	92.41	.00034

(f) $R = 3.15 \times 10^6$; $T_t = 1392^\circ$ R; $p_t = 725$ psia; $M_\infty = 7.93$

x, in.	q, Btu/sec-ft^2	T_w, $^\circ$F	h, Btu/sec-ft^2-$^\circ$F
	y = 0.05 in.		
0.50	1.68831	113.24	0.00255
.75	1.38643	98.39	.00205
1.00	1.18824	96.05	.00175
1.50	.97563	93.56	.00143
2.25	.59972	90.86	.00087
3.25	.45875	91.60	.00067
4.50	-------	------	-------
6.00	.24408	88.72	.00035
7.75	.20317	88.77	.00030
9.75	.09795	86.26	.00013
	y = 0.15 in.		
0.50	1.64696	110.93	0.00248
.75	1.27170	97.10	.00188
1.00	1.10138	95.32	.00162
1.50	.99801	102.61	.00148
2.25	.66884	97.48	.00099
3.25	.71191	92.95	.00105
4.50	.40036	90.20	.00058
6.00	.38951	93.25	.00057
7.75	.37873	90.02	.00055
9.75	.28081	92.68	.00041
	y = 0.35 in.		
0.50	1.56191	110.70	0.00235
.75	1.15364	103.44	.00172
1.00	.91613	94.58	.00135
1.50	.79859	98.08	.00118
2.25	.73859	99.35	.00109
3.25	.73364	98.98	.00108
4.50	.66078	99.63	.00098
6.00	.64750	93.63	.00095
7.75	.56551	96.11	.00083
9.75	.45810	96.54	.00067
	y = 0.60 in.		
0.50	1.60334	113.19	0.00242
.75	1.34594	107.25	.00201
1.00	1.03916	96.37	.00153
1.50	.85168	94.11	.00125
2.25	.60915	97.39	.00090
3.25	.52891	94.95	.00077
4.50	.53356	92.72	.00078
6.00	.56952	93.40	.00083
7.75	.53610	96.02	.00079
9.75	.48059	93.74	.00071
	y = 1.00 in.		
0.50	1.52225	112.57	0.00230
.75	1.21682	99.49	.00180
1.00	1.02053	97.45	.00151
1.50	.88564	95.76	.00130
2.25	.68159	94.97	.00100
3.25	.52344	96.42	.00077
4.50	.41524	96.06	.00061
6.00	.38313	91.92	.00056
7.75	.42270	95.03	.00062
9.75	.41564	96.72	.00062
	y = 1.50 in.		
0.50	1.53402	103.12	0.00228
.75	1.19533	107.50	.00179
1.00	1.03543	103.88	.00155
1.50	.85058	96.22	.00126
2.25	.65629	101.01	.00097
3.25	.55597	98.43	.00082
4.50	.46677	94.19	.00069
6.00	.37766	96.59	.00056
7.75	.36910	92.67	.00054
9.75	.38647	94.85	.00057
	y = 2.00 in.		
0.50	1.54730	107.61	0.00232
.75	1.27703	104.28	.00190
1.00	1.10767	102.42	.00165
1.50	.91956	100.21	.00136
2.25	.74082	96.89	.00109
3.25	.63446	95.12	.00093
4.50	.52036	94.71	.00076
6.00	.42399	94.76	.00062
7.75	.40479	96.81	.00060
9.75	.45788	99.44	.00068

(g) $R = 10.07 \times 10^6$; $T_t = 1467^\circ$ R; $p_t = 2510$ psia; $M_\infty = 8.0$

x, in.	q, Btu/sec-ft^2	T_w, $^\circ$F	h, Btu/sec-ft^2-$^\circ$F
	y = 0.05 in.		
0.50	3.72948	115.28	0.00516
.75	2.75564	110.62	.00379
1.00	2.34176	107.15	.00320
1.50	1.87214	104.03	.00255
2.25	1.04051	100.00	.00141
3.25	.88400	102.78	.00120
4.50	.13662	79.02	.00018
6.00	.47179	98.71	.00064
7.75	.45977	97.04	.00062
9.75	.52759	95.22	.00071
	y = 0.15 in.		
0.50	3.24096	112.93	0.00447
.75	2.49640	109.45	.00342
1.00	2.24977	107.54	.00308
1.50	2.00339	121.20	.00279
2.25	1.72469	105.29	.00236
3.25	1.42793	102.48	.00194
4.50	.74798	104.81	.00102
6.00	.81768	105.49	.00111
7.75	.84123	97.48	.00114
9.75	.83055	104.52	.00113
	y = 0.35 in.		
0.50	2.93024	113.14	0.00404
.75	2.04174	108.05	.00280
1.00	1.74474	105.85	.00238
1.50	1.51715	112.71	.00209
2.25	1.51356	103.99	.00206
3.25	1.55390	105.30	.00212
4.50	1.34300	103.84	.00183
6.00	1.19490	102.78	.00162
7.75	1.09803	100.15	.00149
9.75	.88516	99.90	.00119
	y = 0.60 in.		
0.50	3.10556	114.84	0.00429
.75	-------	------	-------
1.00	2.08627	107.46	.00285
1.50	1.68529	104.20	.00230
2.25	1.18331	101.77	.00160
3.25	.97137	99.63	.00132
4.50	-------	------	-------
6.00	.86077	99.45	.00117
7.75	1.05230	100.17	.00143
9.75	.95960	100.36	.00180
	y = 1.00 in.		
0.50	2.91540	113.74	0.00402
.75	2.35903	109.88	.00324
1.00	2.14723	107.84	.00294
1.50	1.71379	104.39	.00233
2.25	1.32315	102.86	.00180
3.25	1.03208	99.92	.00140
4.50	.83846	100.51	.00114
6.00	.74535	105.63	.00102
7.75	.91254	99.74	.00124
9.75	1.32618	101.87	.00180
	y = 1.50 in.		
0.50	2.87386	110.97	0.00396
.75	2.40453	108.02	.00329
1.00	2.05841	105.77	.00281
1.50	1.67682	102.42	.00228
2.25	1.37387	101.65	.00186
3.25	1.16576	99.66	.00158
4.50	.91611	100.01	.00124
6.00	.84179	99.96	.00114
7.75	1.04082	100.25	.00141
9.75	2.19916	107.49	.00300
	y = 2.00 in.		
0.50	2.94411	113.33	0.00406
.75	2.41869	110.61	.00332
1.00	-------	------	-------
1.50	1.83403	105.65	.00250
2.25	1.49223	101.05	.00202
3.25	1.25311	99.24	.00170
4.50	1.04032	99.60	.00141
6.00	1.08914	101.74	.00148
7.75	1.90754	118.53	.00265
9.75	3.38590	112.25	.00471

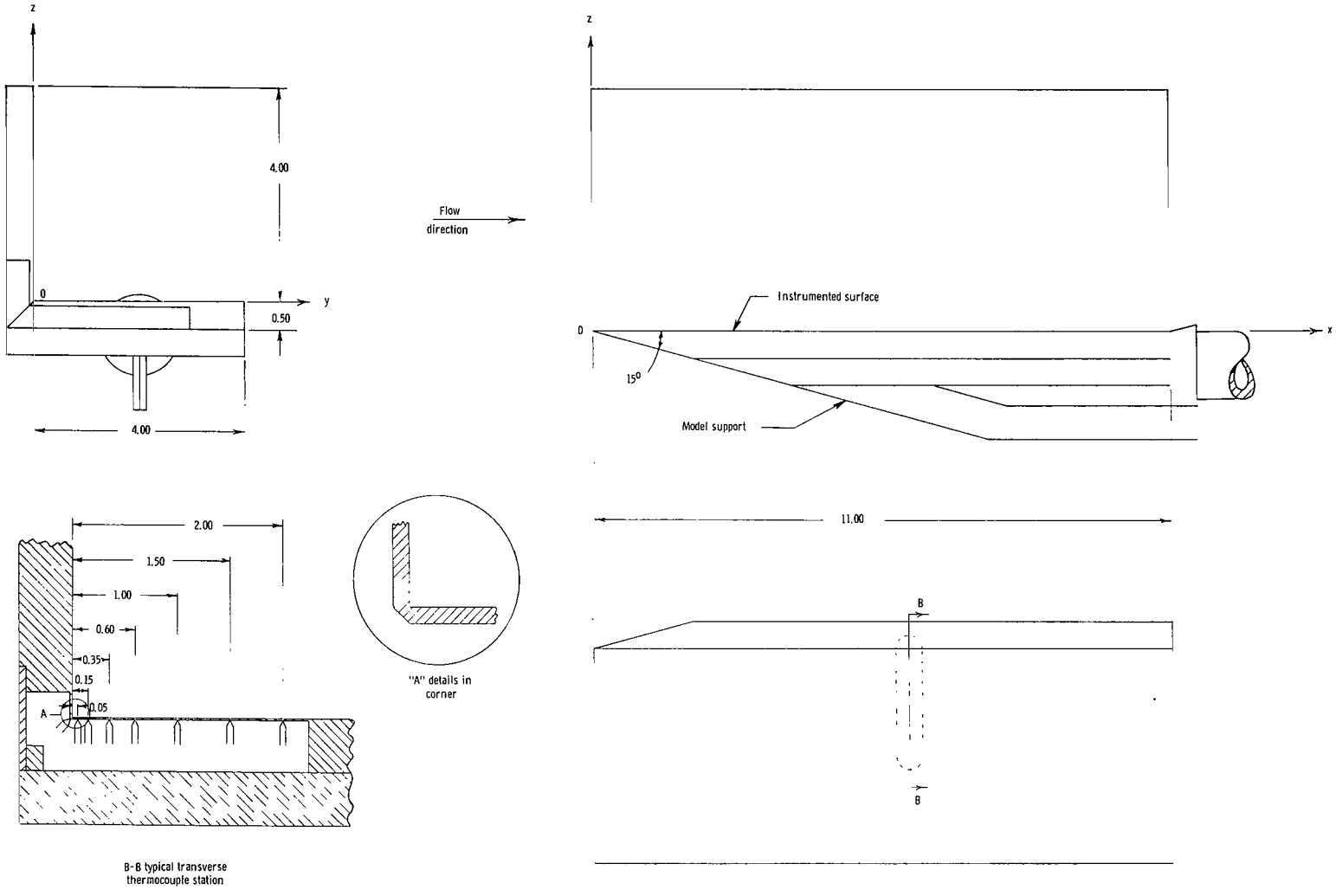

Figure 1.- General model dimensions. All dimensions are in inches except as noted.

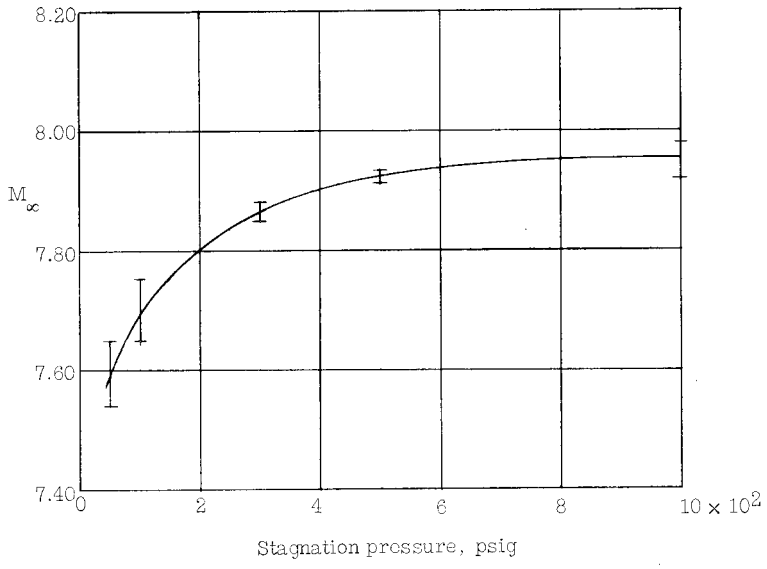

Figure 2.- Tunnel-test-section Mach number variation with stagnation pressure.

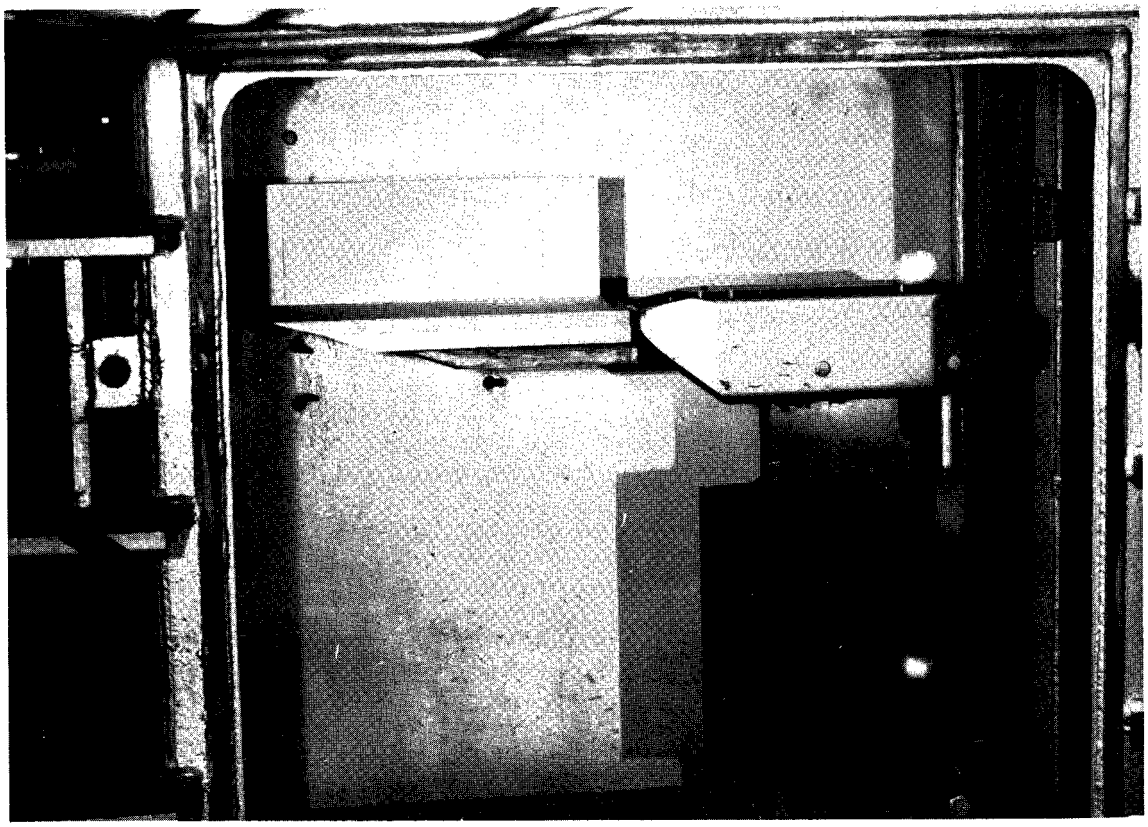

L-64-3094

Figure 3.- Temperature-sensitive-paint corner model on test-section injection mechanism.

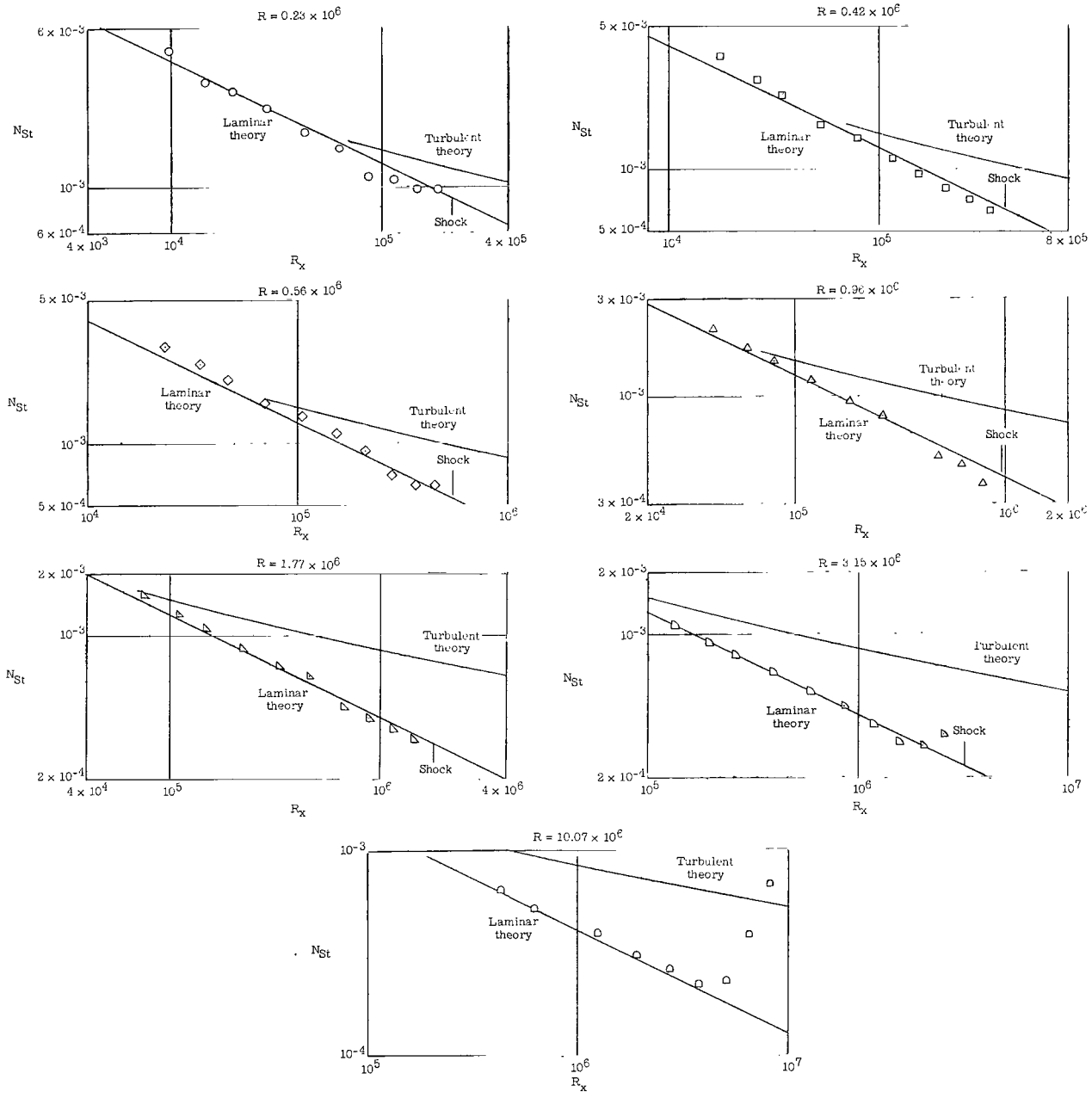

(a) y = 2.00 in.

Figure 4.- Stanton number variation along model for various distances from the corner.

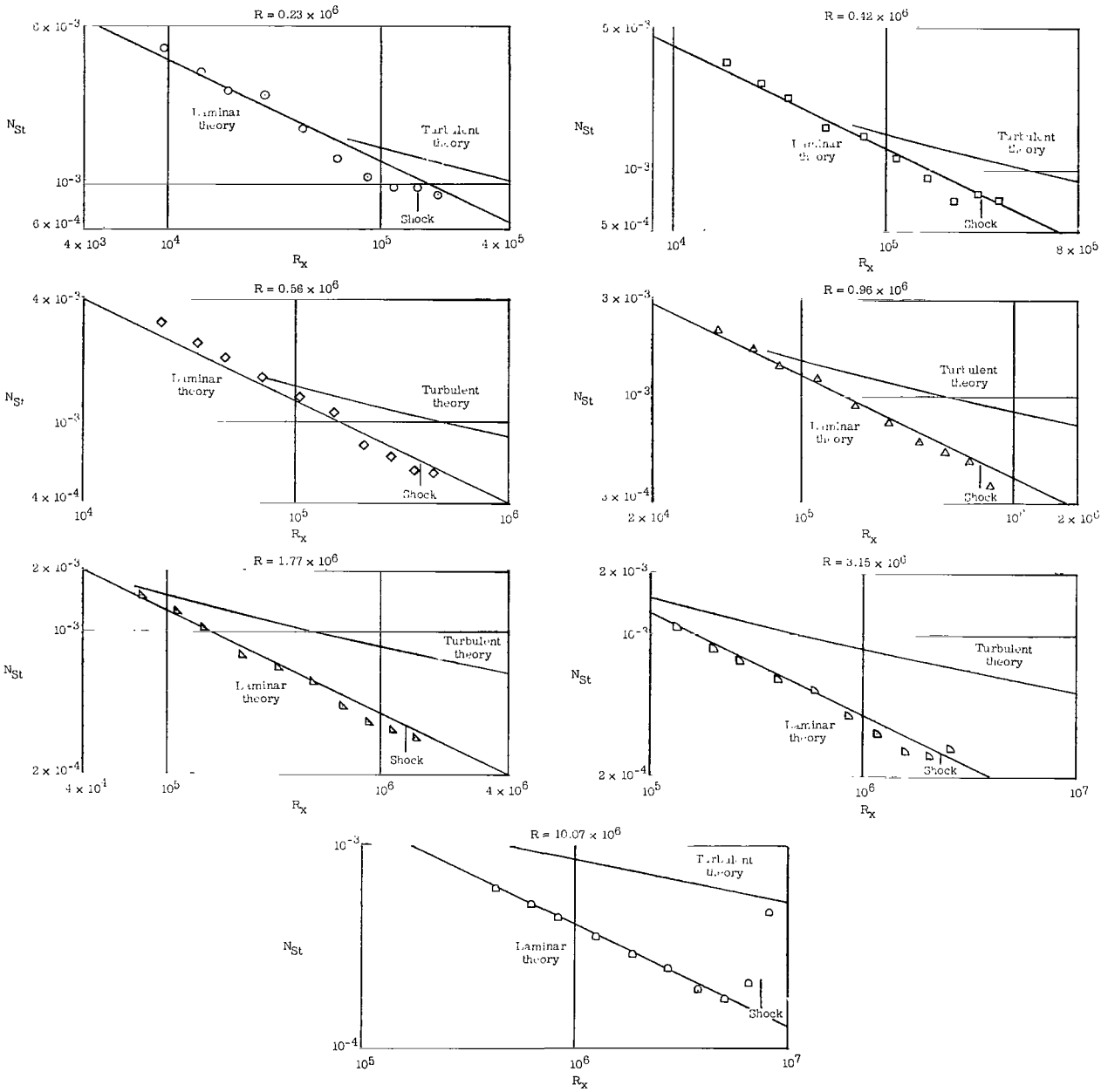

(b) y = 1.50 in.

Figure 4.- Continued.

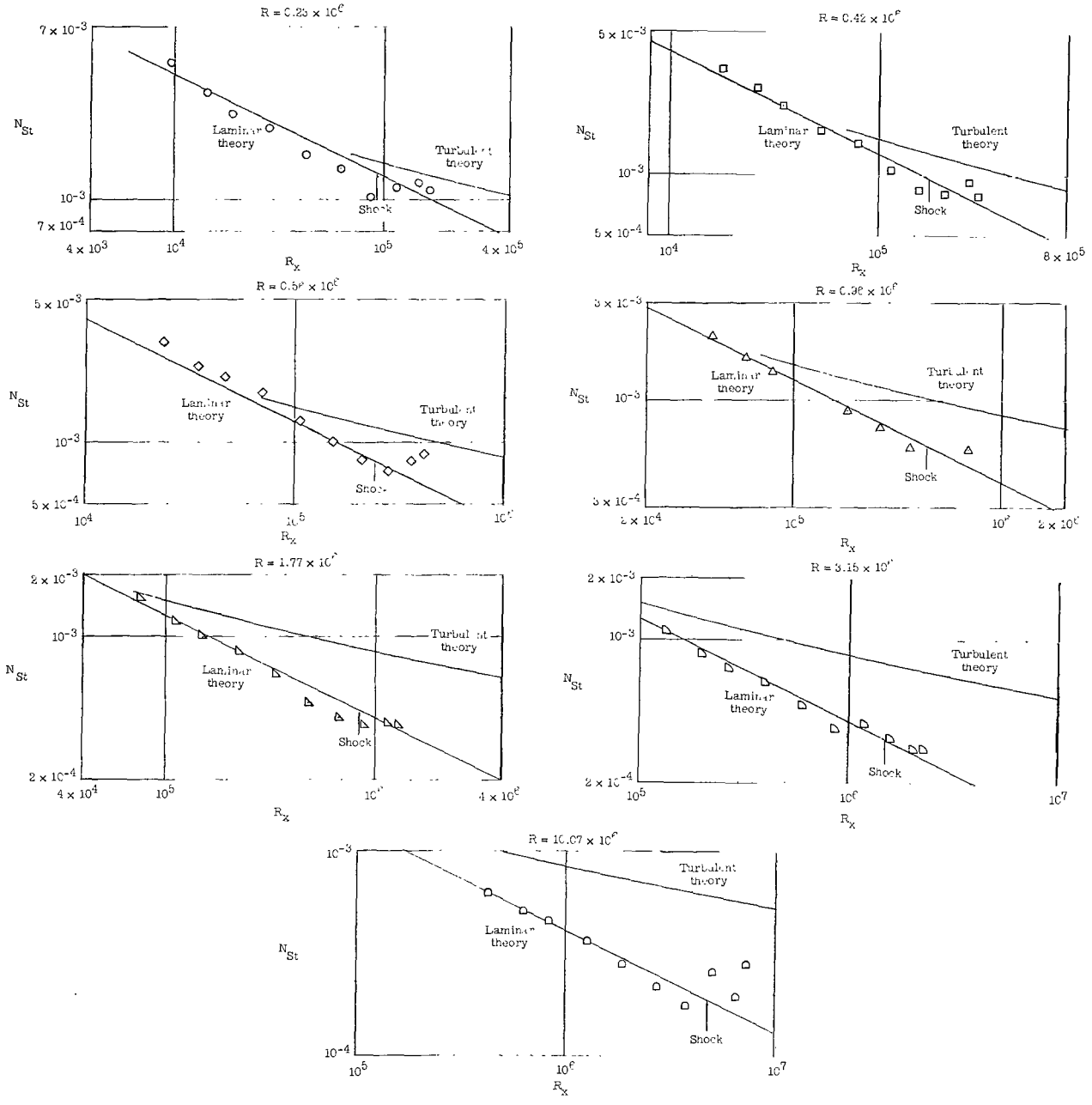

(c) y = 1.00 in.

Figure 4.- Continued.

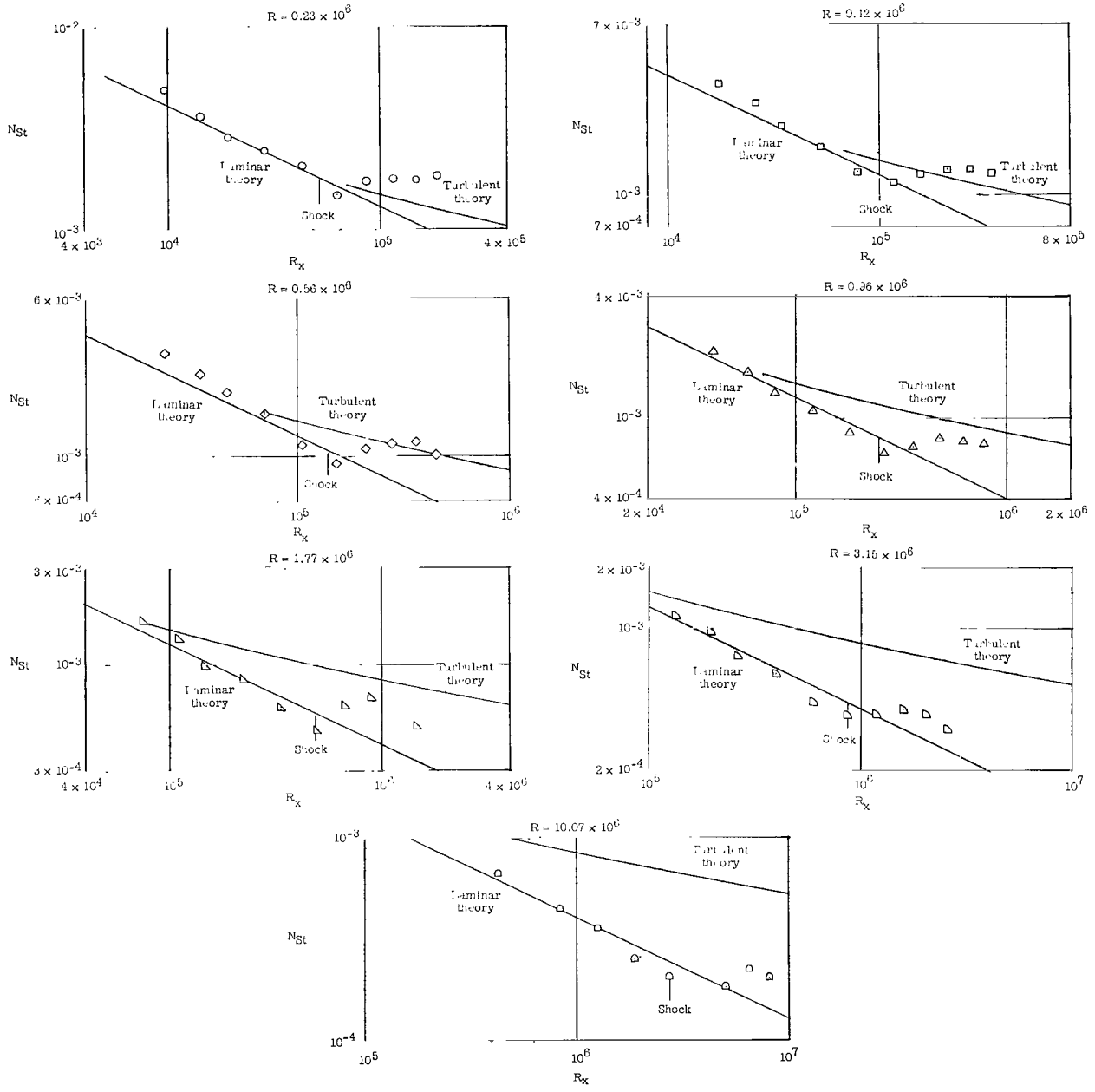

(d) y = 0.60 in.

Figure 4.- Continued.

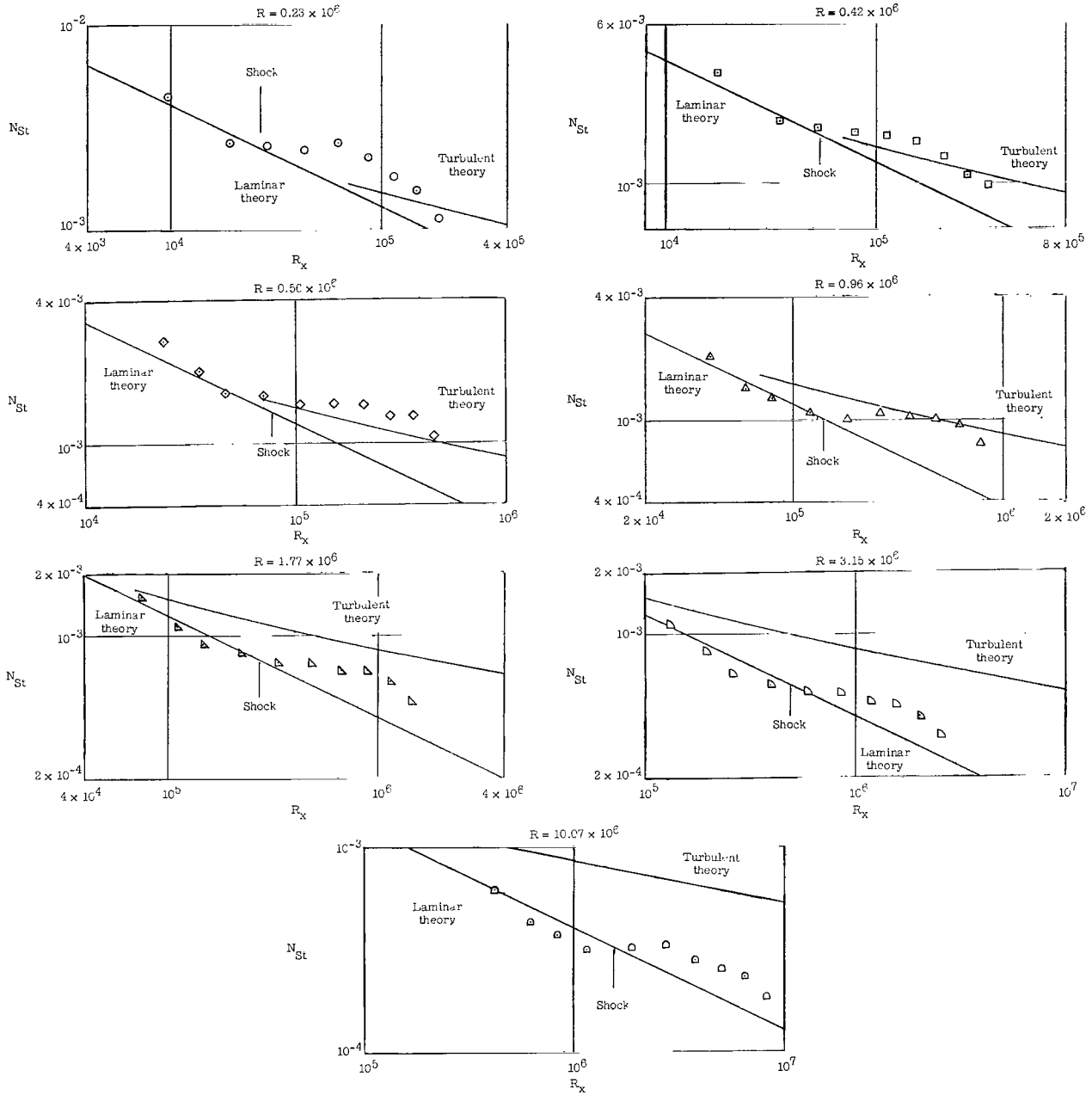

(e) y = 0.35 in.

Figure 4.- Continued.

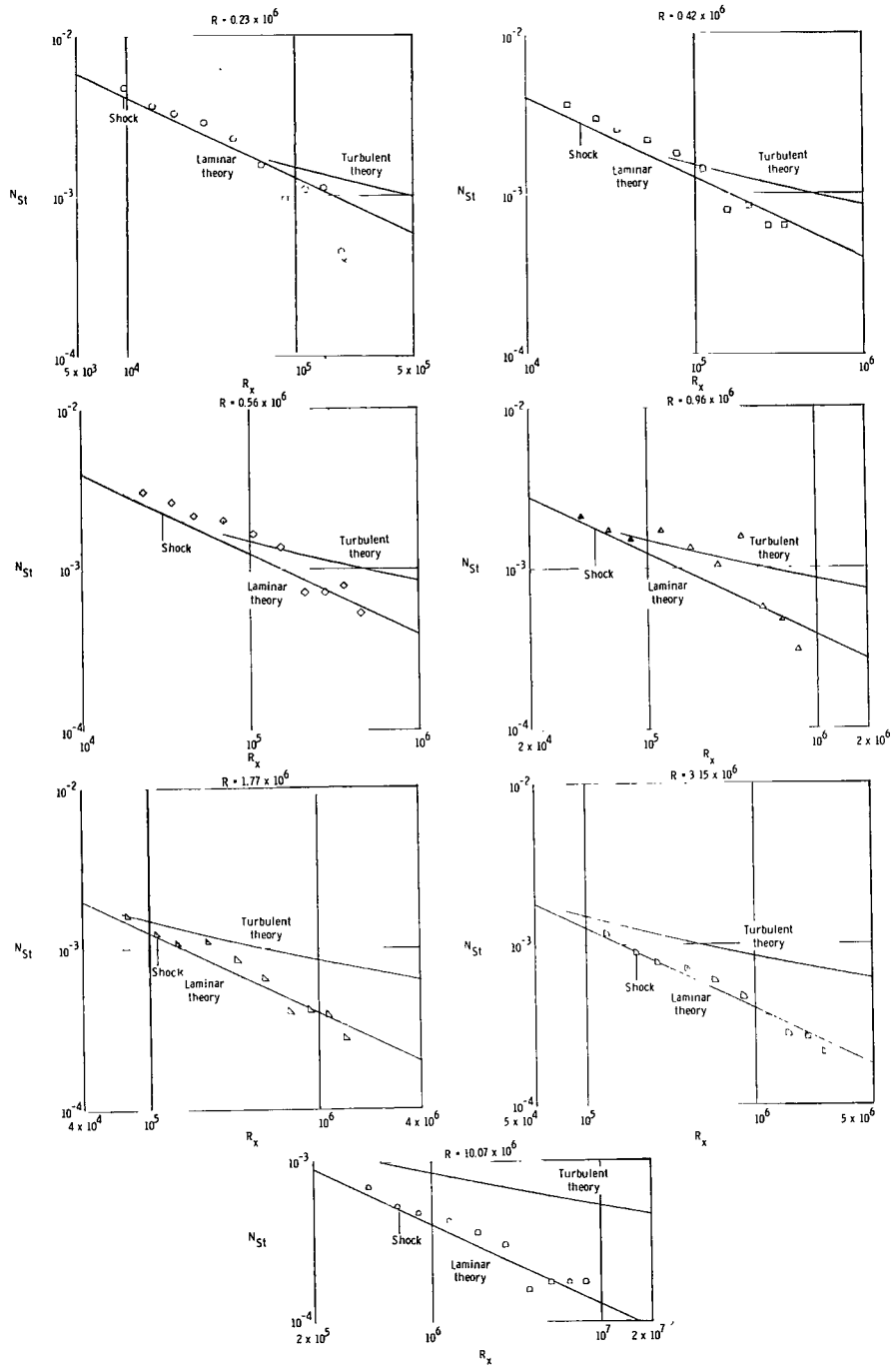

(f) y = 0.15 in.

Figure 4.- Continued.

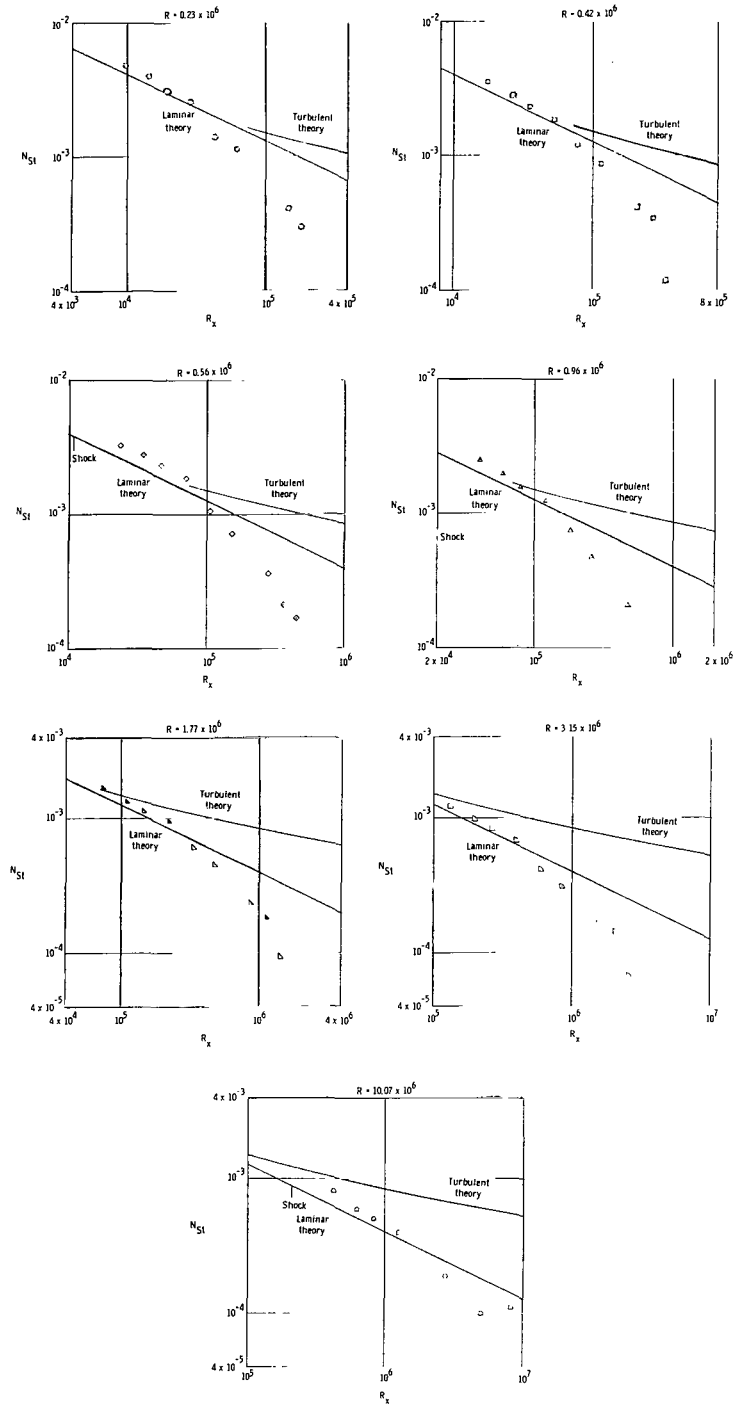

(g) y = 0.05 in.

Figure 4.- Concluded.

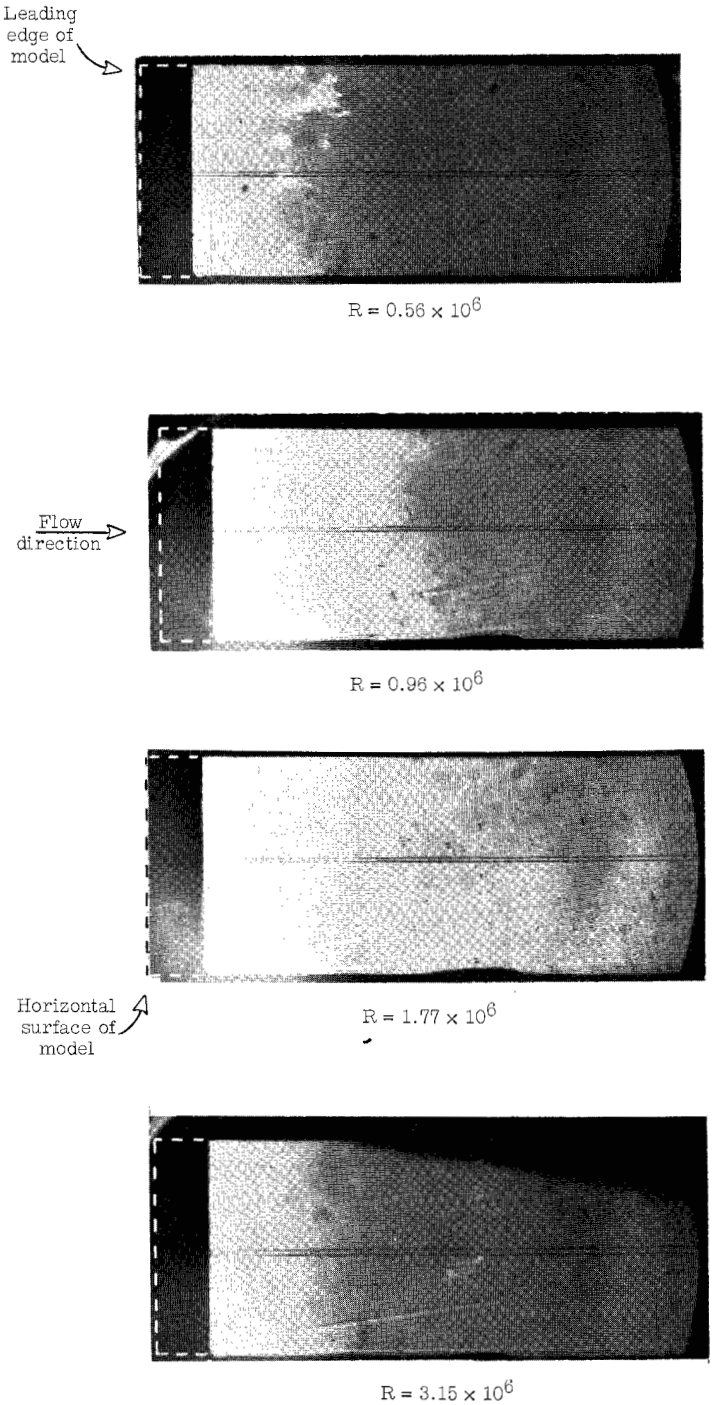

L-64-3095

(a) Shadowgraphs of flow over corner model.

Figure 5.- Shadowgraph study.

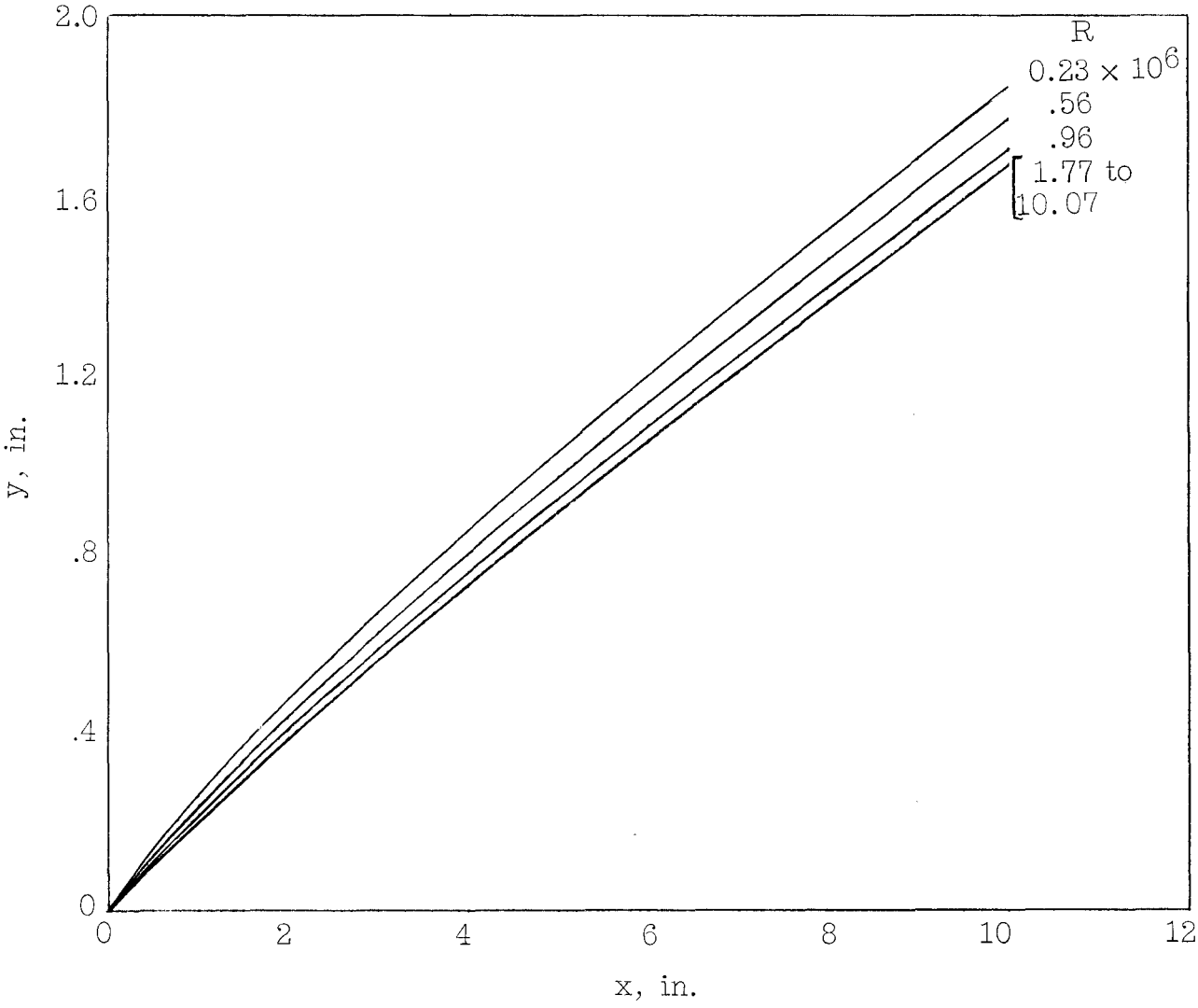

(b) Shock location as obtained from shadowgraph results.

Figure 5.- Concluded.

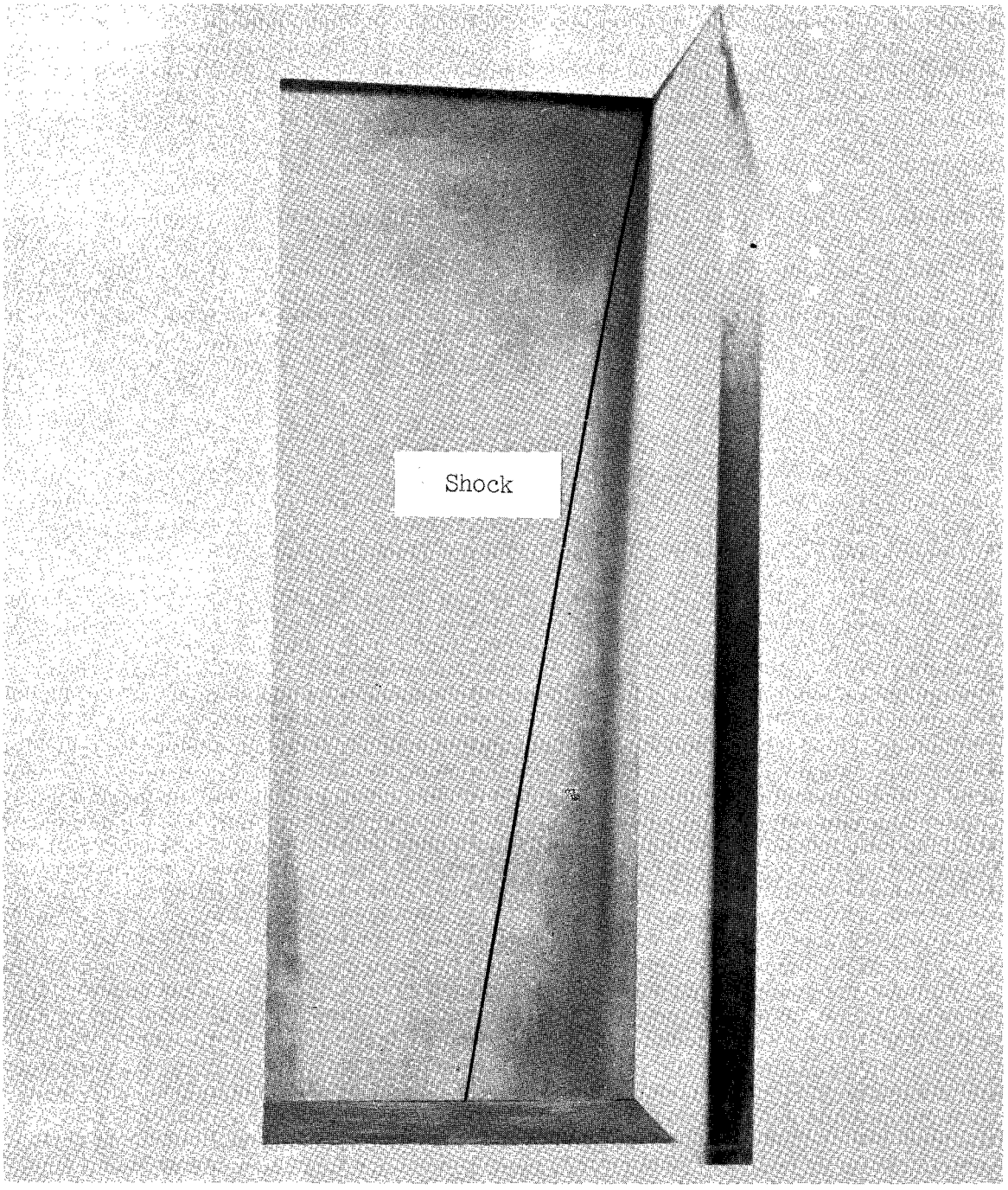

Figure 6.- Corner-flow-model temperature-sensitive-paint results. $R = 1.77 \times 10^6$. L-64-3096

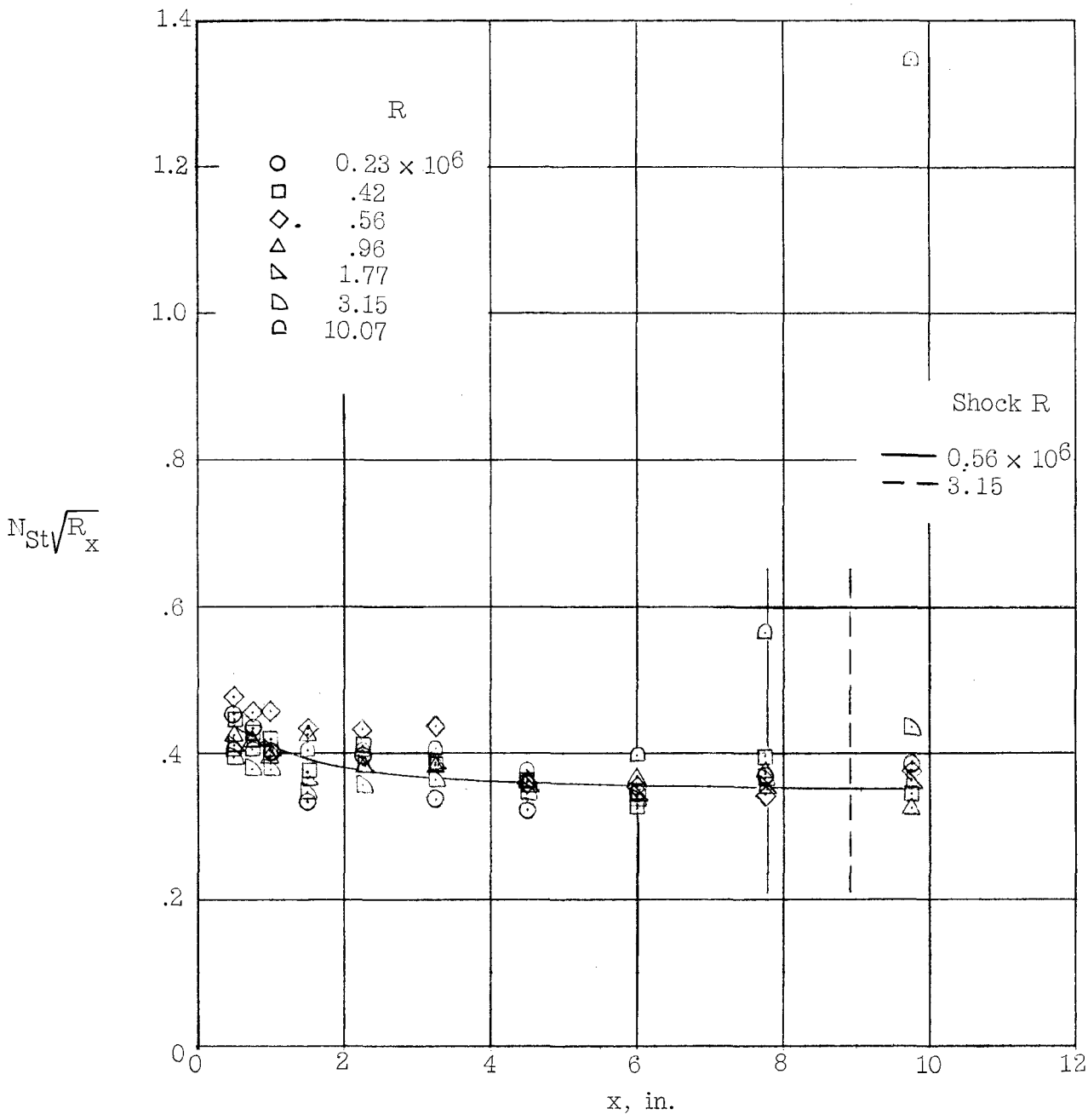

(a) y = 1.50 in.

Figure 7.- Heat-transfer-parameter variation along model for various distances from corner.

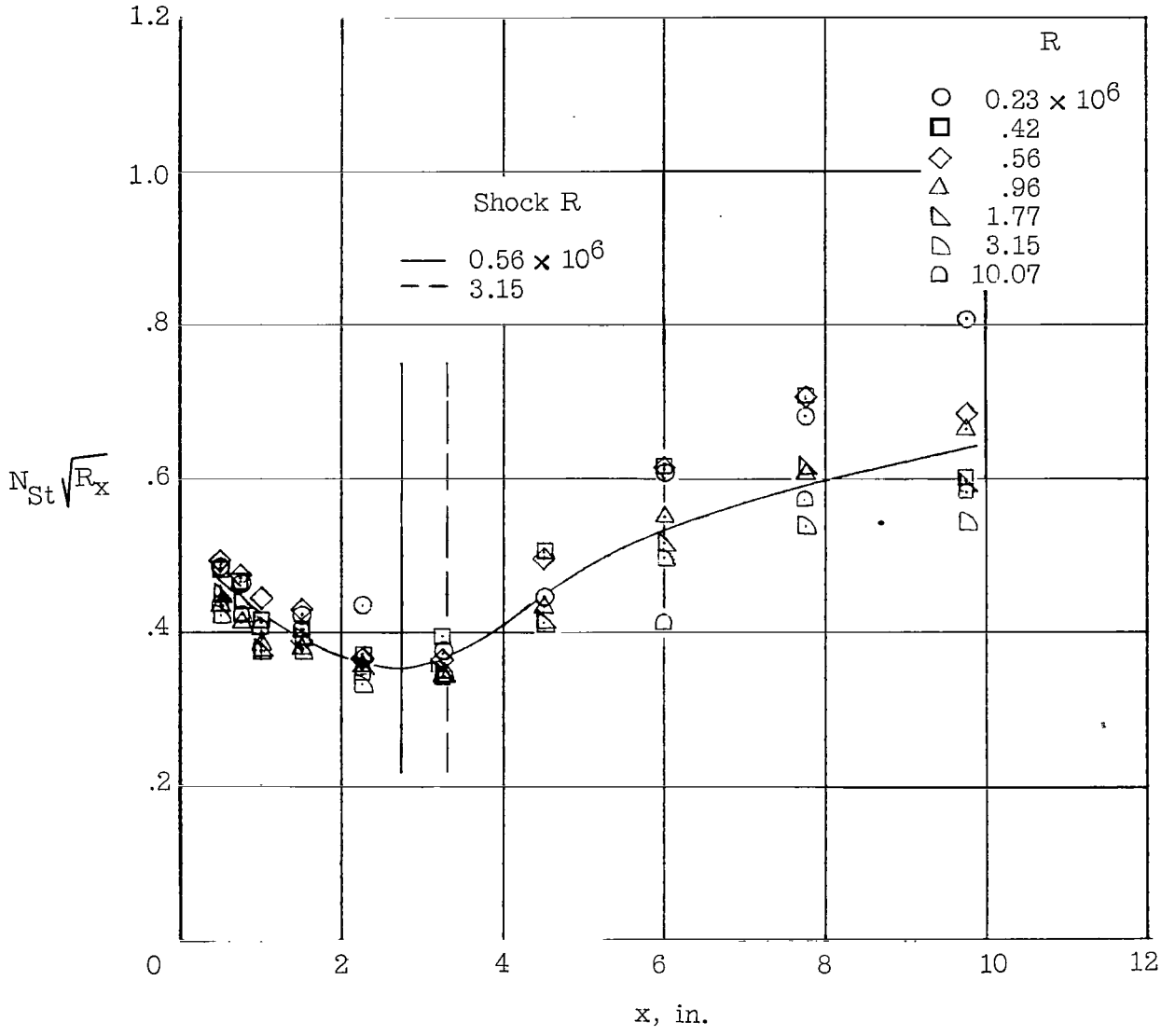

(b) y = 0.60 in.

Figure 7.- Continued.

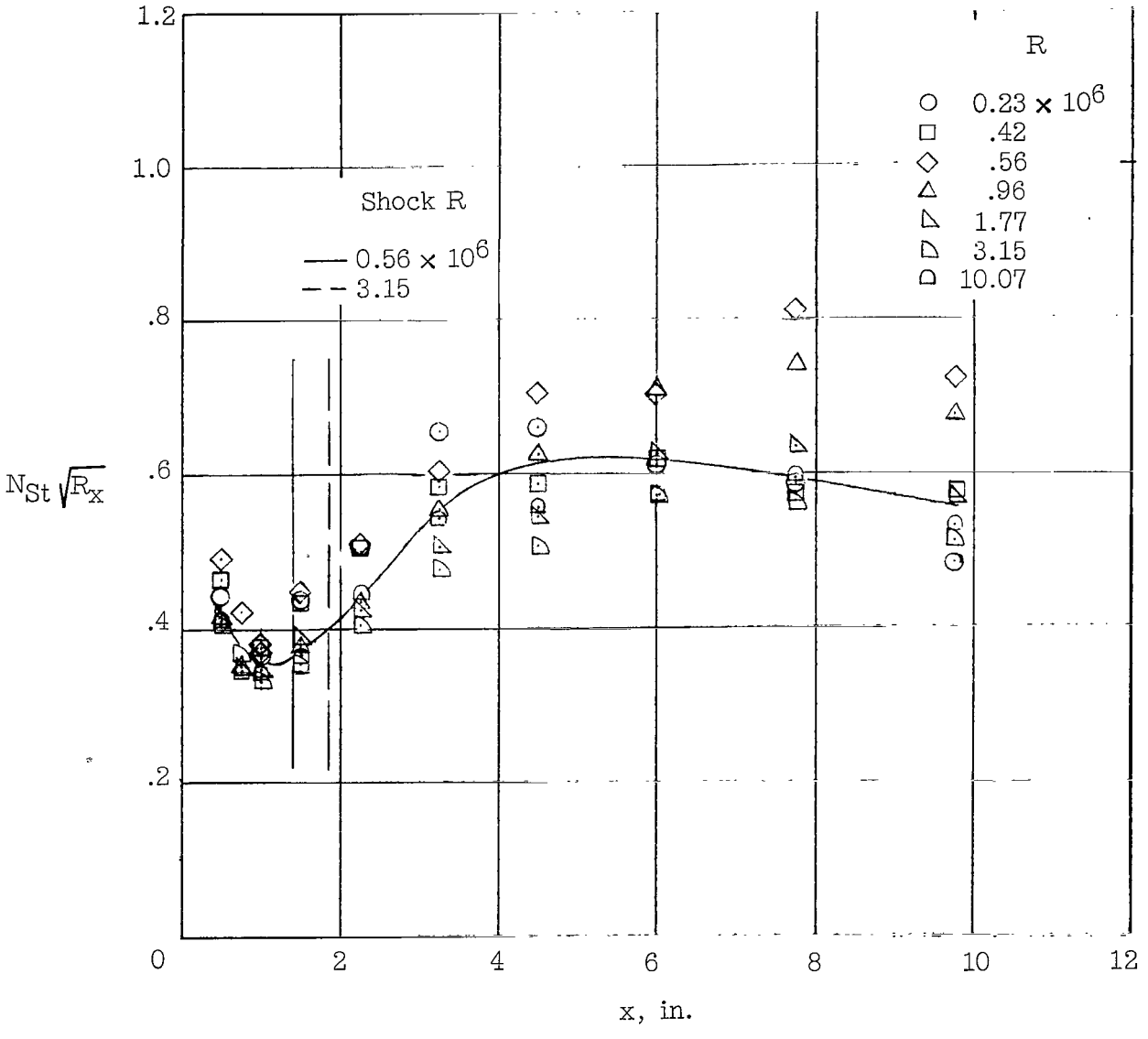

(c) y = 0.35 in.

Figure 7.- Concluded.

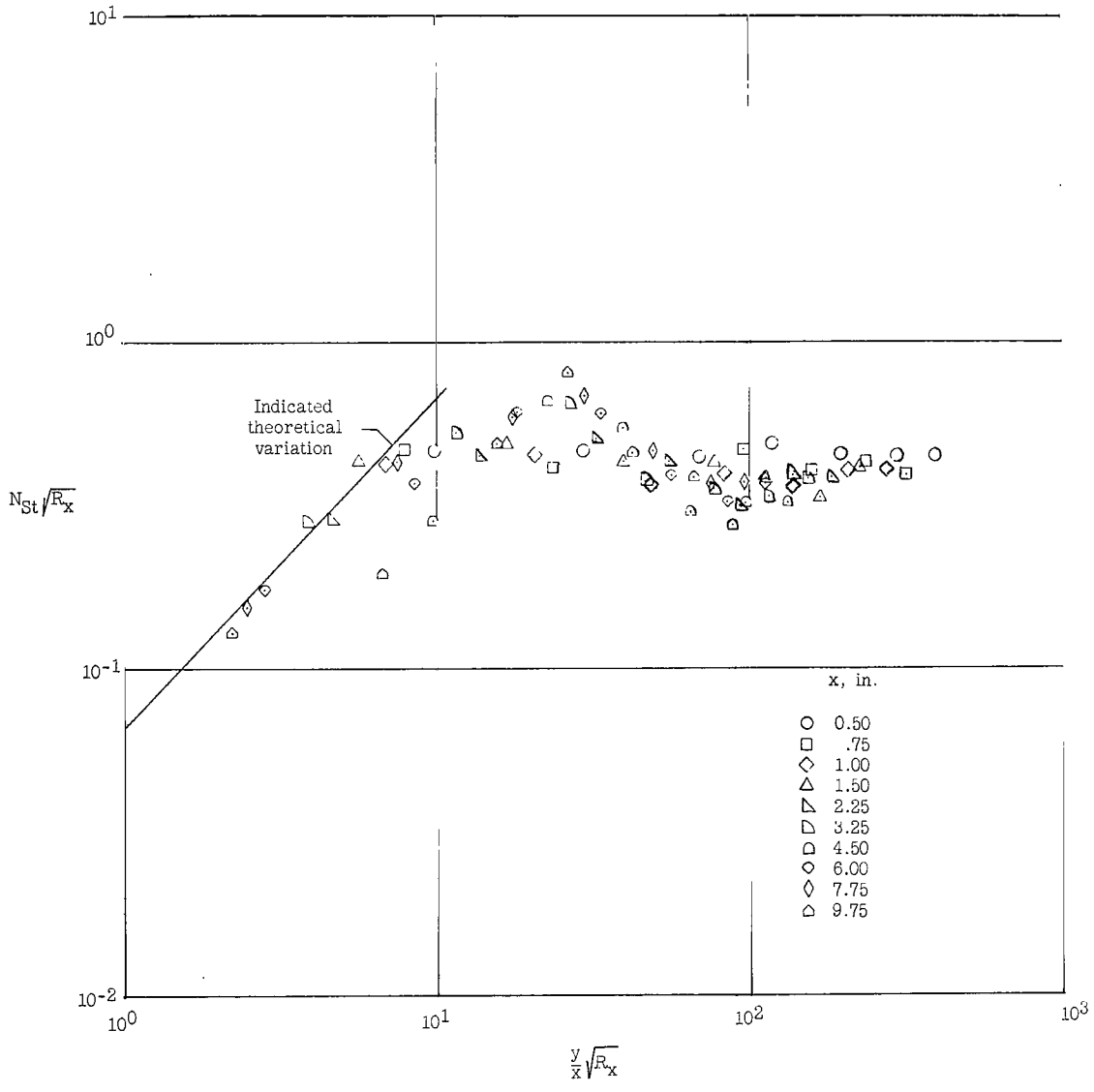

(a) $R = 0.23 \times 10^6$.

Figure 8.- Heat-transfer parameter in the mutual boundary-layer interaction region.

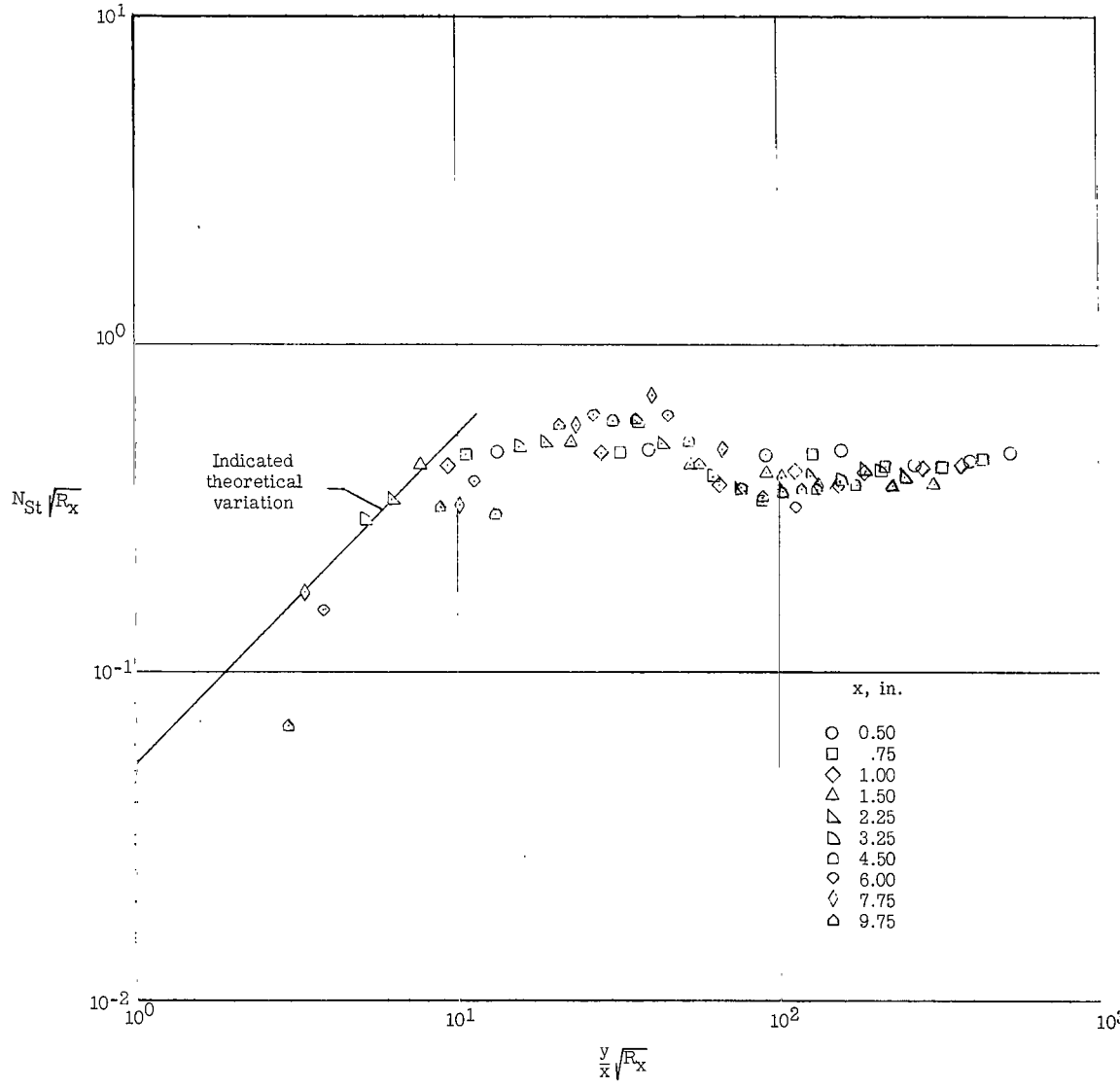

(b) $R = 0.42 \times 10^6$.

Figure 8.- Continued.

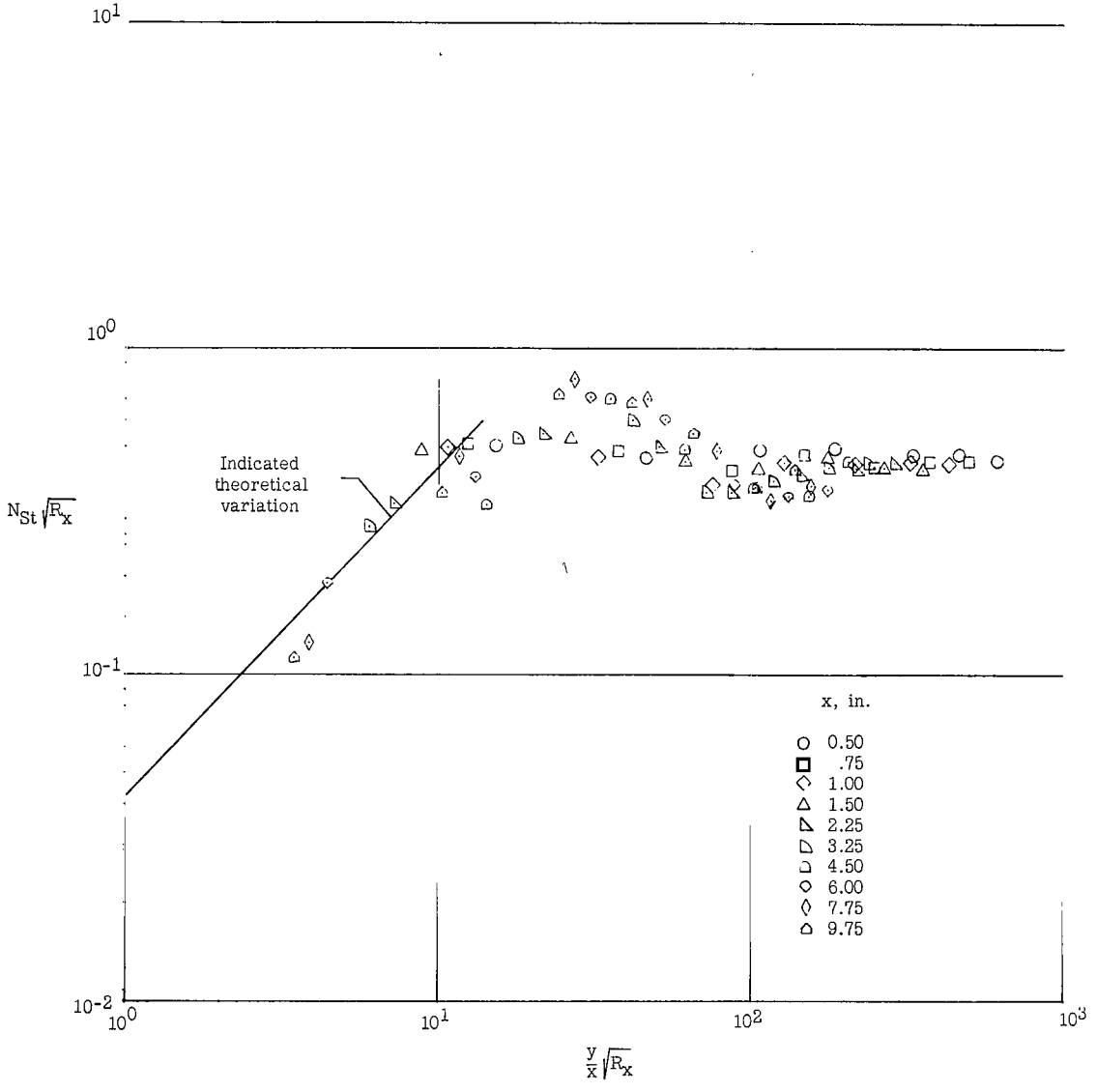

(c) $R = 0.56 \times 10^6$.

Figure 8.- Continued.

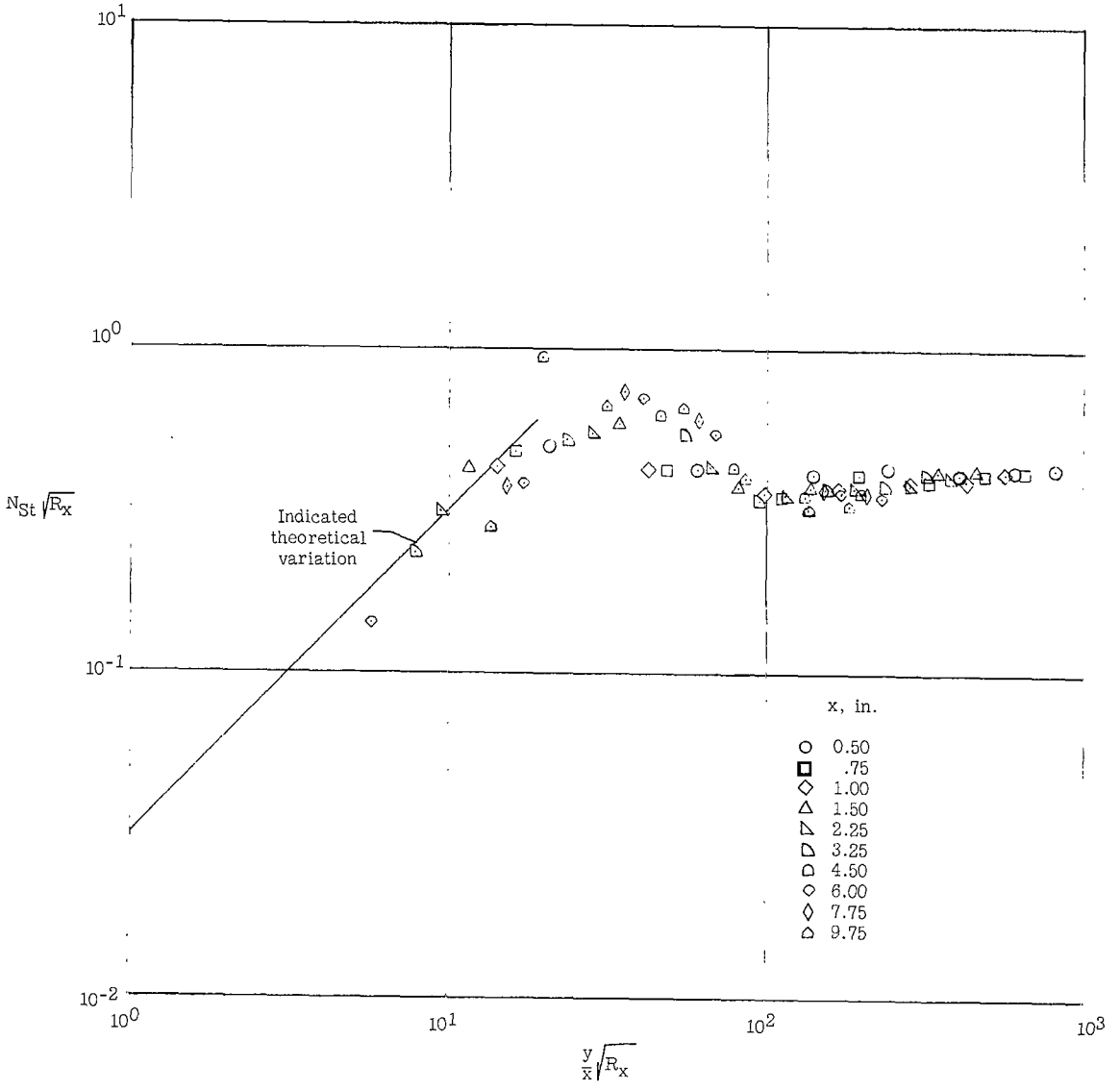

(a) $R = 0.96 \times 10^6$.

Figure 8.- Continued.

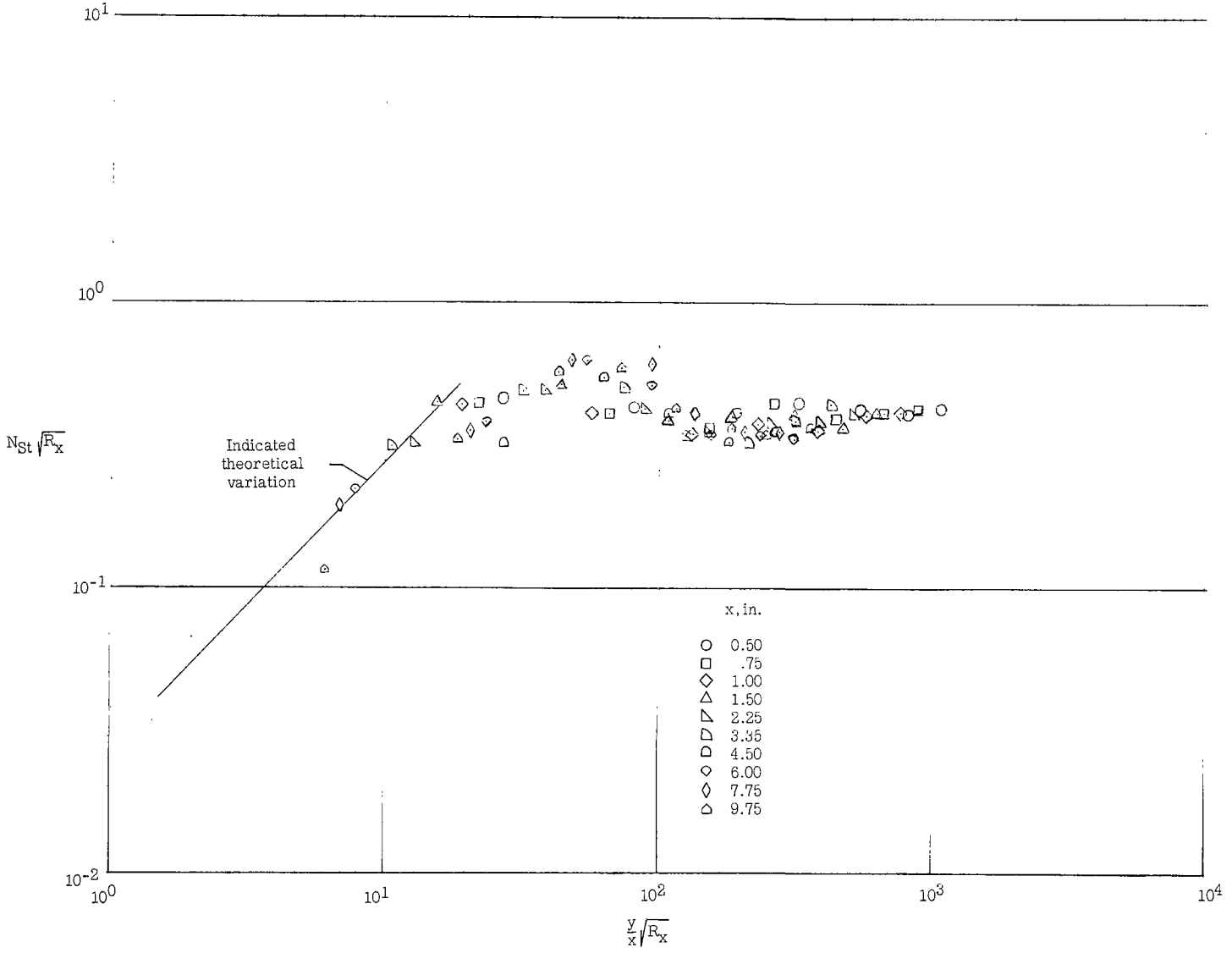

(e) $R = 1.77 \times 10^6$.

Figure 8.- Continued.

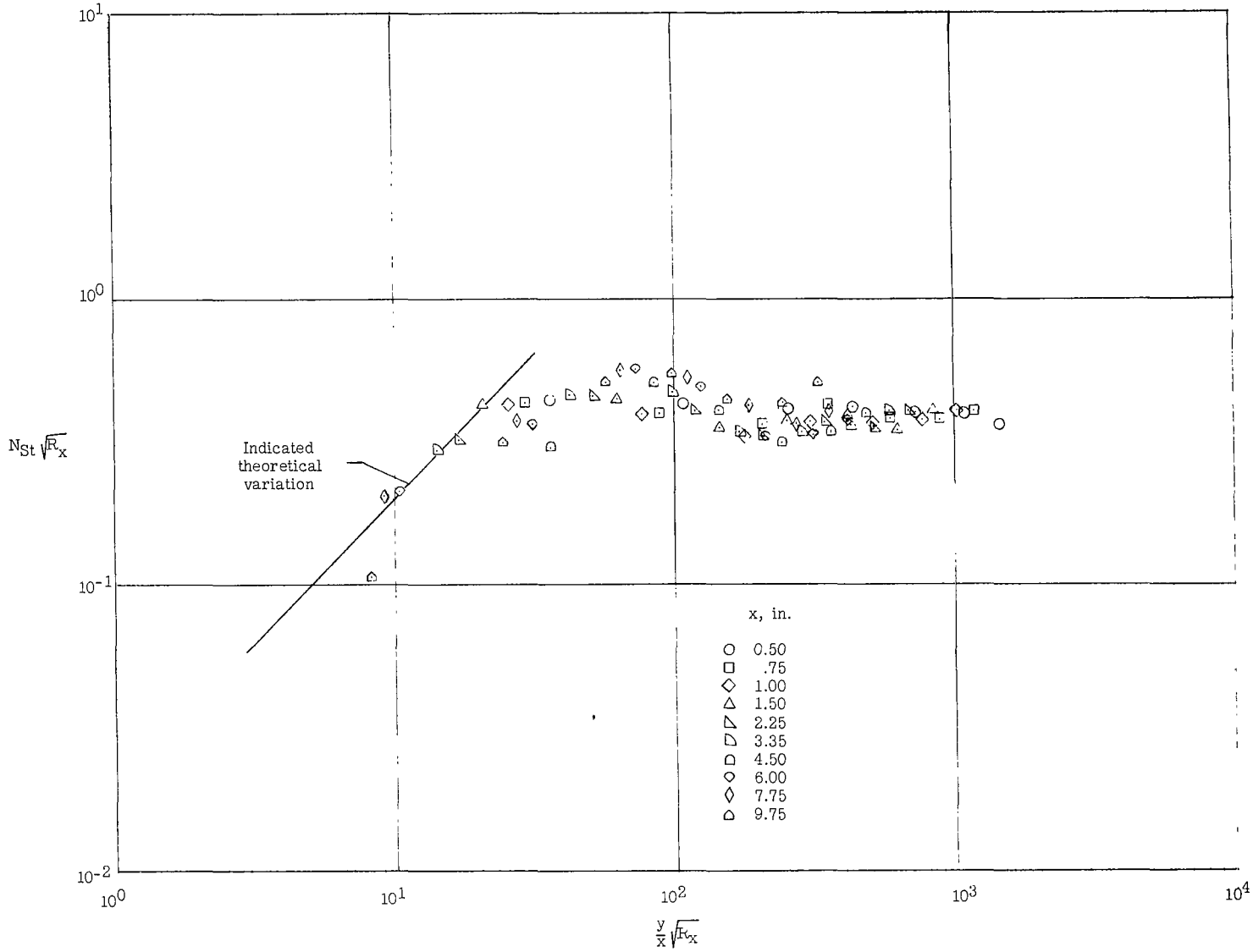

(f) $R = 3.15 \times 10^6$.

Figure 8.- Continued.

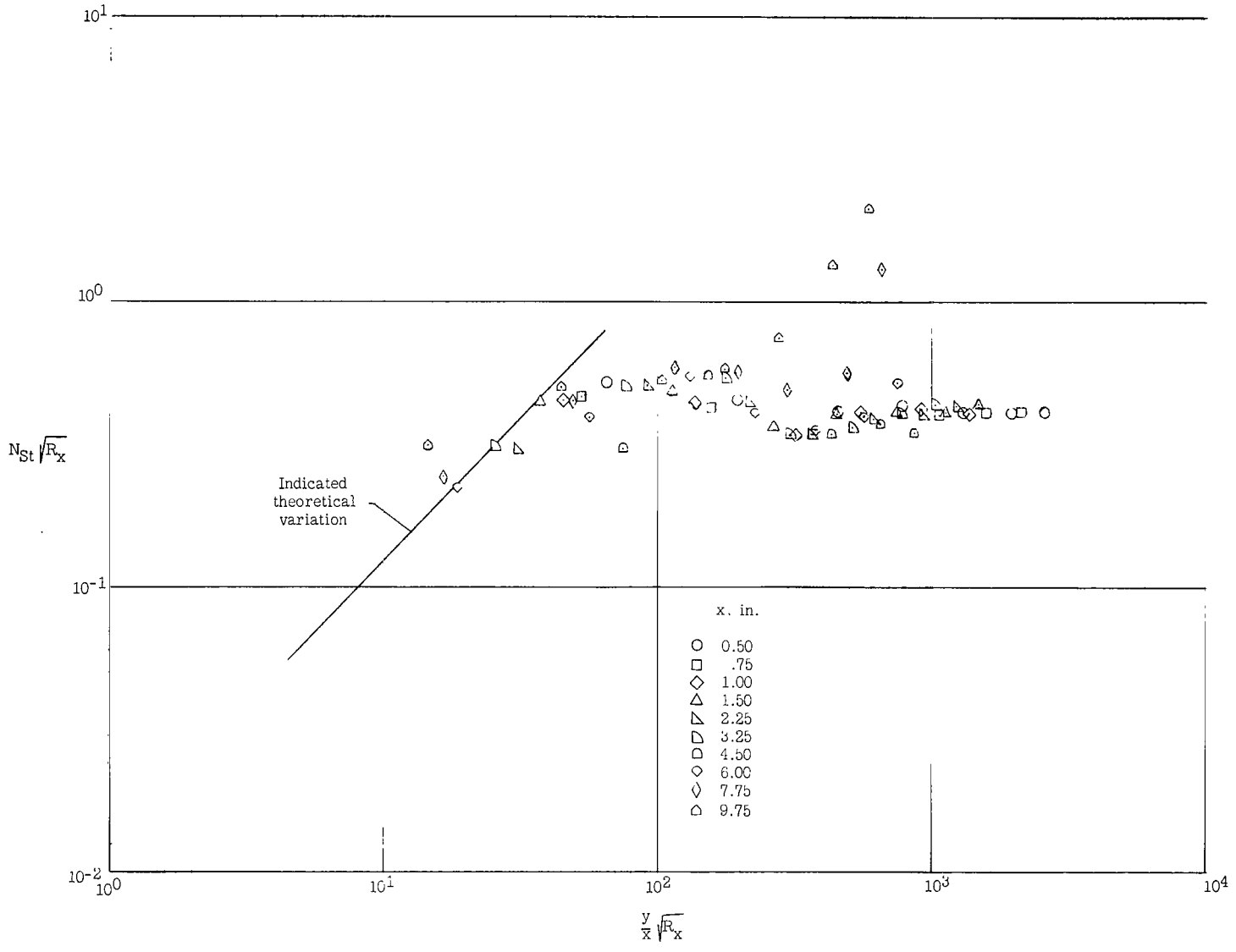

(g) $R = 10.07 \times 10^6$.

Figure 8.- Concluded.

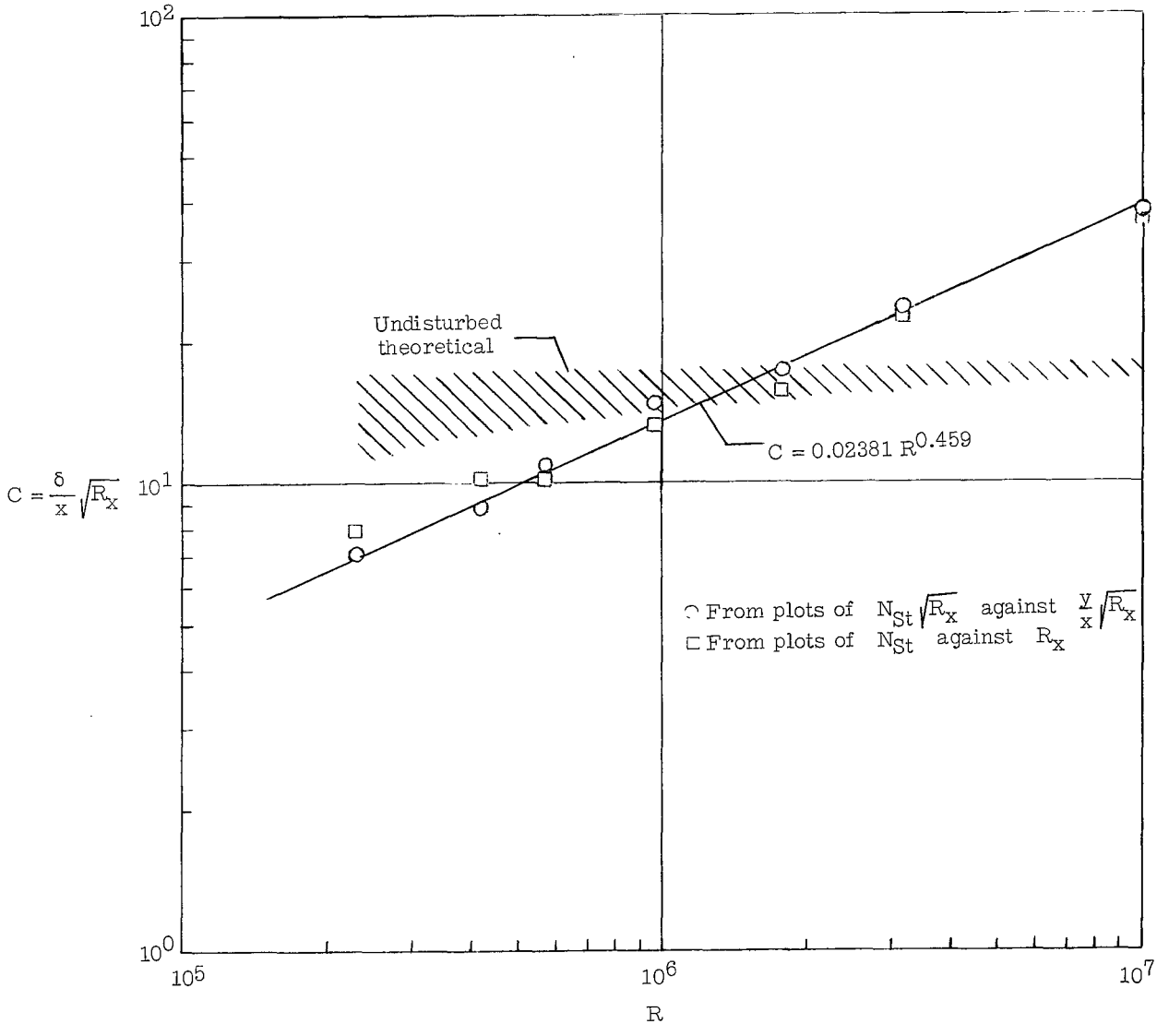

Figure 9.- Nondimensional boundary-layer-interaction parameter variation with unit Reynolds number.

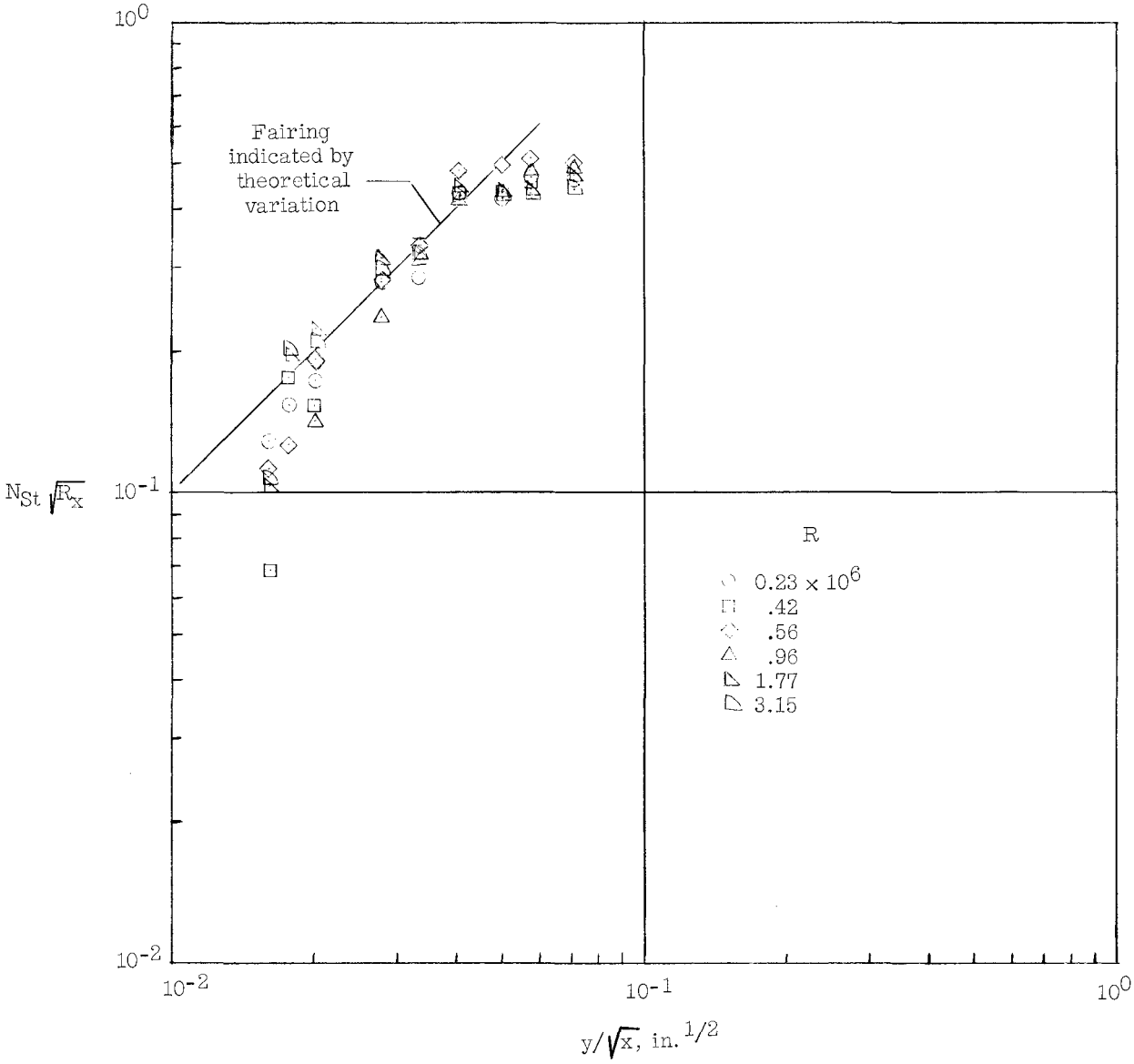

Figure 10.- Correlation of heat-transfer parameter in mutual-boundary-layer-interaction region. y = 0.05 in.

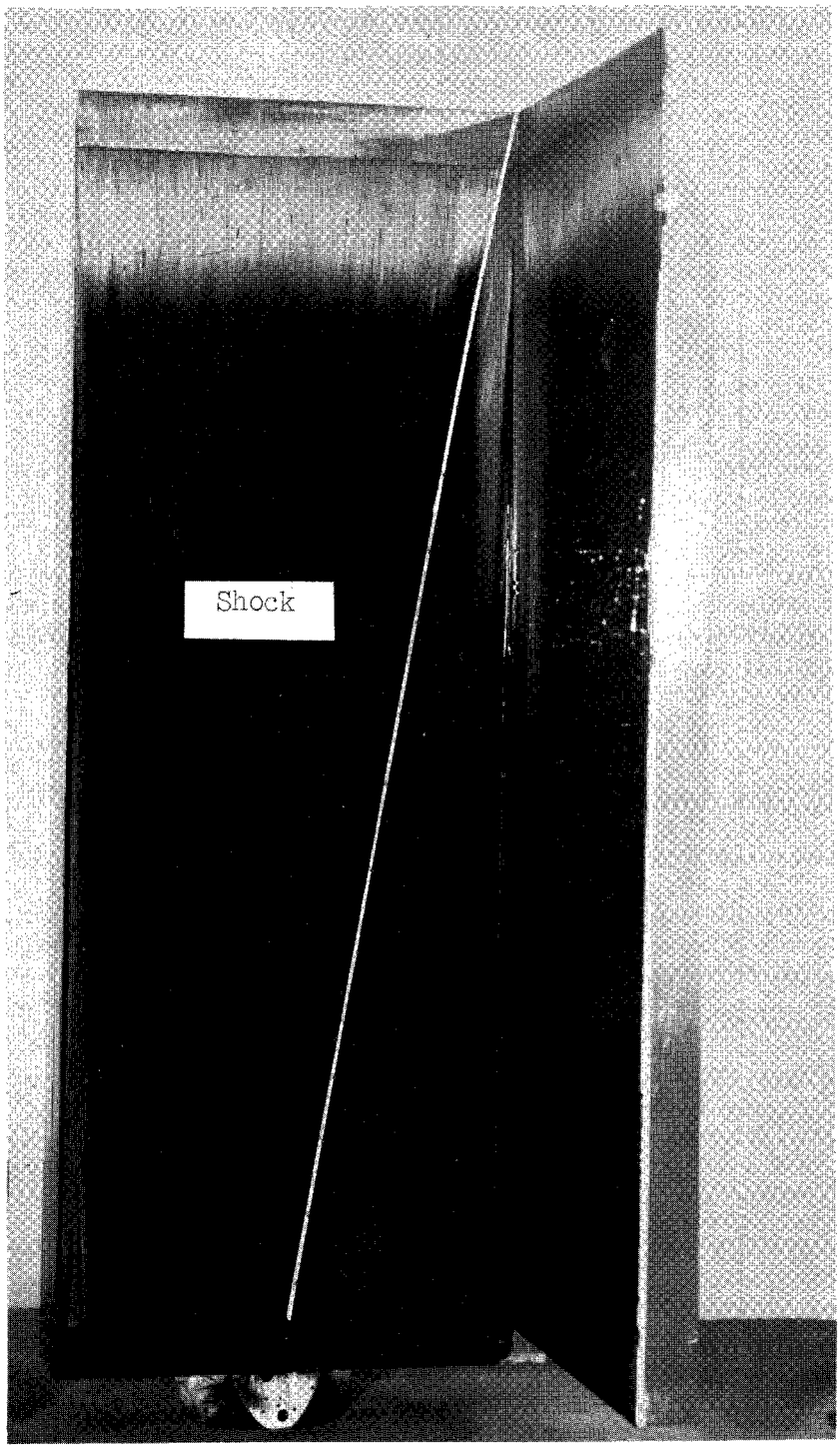

(a) Completely coated technique. L-64-3097

Figure 11.- Corner-flow model; oil-flow results. $R = 1.77 \times 10^6$.

(b) Closeup of completely coated technique. L-64-3098

Figure 11.- Continued.

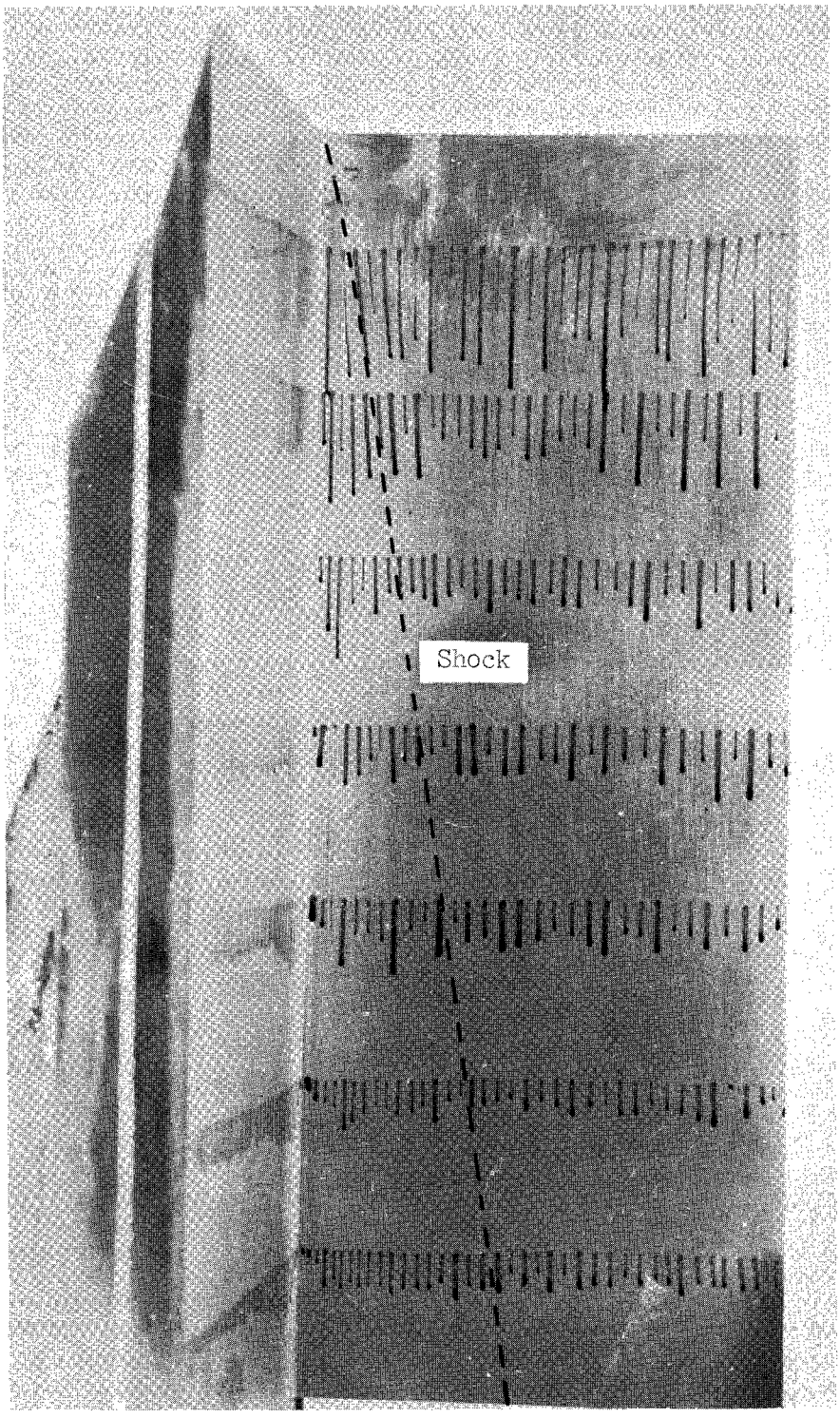

(c) Discrete-dot technique. L-64-3099

Figure 11.- Concluded.

NASA-Langley, 1964 L-3501

2/7/85

"The aeronautical and space activities of the United States shall be conducted so as to contribute . . . to the expansion of human knowledge of phenomena in the atmosphere and space. The Administration shall provide for the widest practicable and appropriate dissemination of information concerning its activities and the results thereof."

—NATIONAL AERONAUTICS AND SPACE ACT OF 1958

NASA SCIENTIFIC AND TECHNICAL PUBLICATIONS

TECHNICAL REPORTS: Scientific and technical information considered important, complete, and a lasting contribution to existing knowledge.

TECHNICAL NOTES: Information less broad in scope but nevertheless of importance as a contribution to existing knowledge.

TECHNICAL MEMORANDUMS: Information receiving limited distribution because of preliminary data, security classification, or other reasons.

CONTRACTOR REPORTS: Technical information generated in connection with a NASA contract or grant and released under NASA auspices.

TECHNICAL TRANSLATIONS: Information published in a foreign language considered to merit NASA distribution in English.

TECHNICAL REPRINTS: Information derived from NASA activities and initially published in the form of journal articles.

SPECIAL PUBLICATIONS: Information derived from or of value to NASA activities but not necessarily reporting the results of individual NASA-programmed scientific efforts. Publications include conference proceedings, monographs, data compilations, handbooks, sourcebooks, and special bibliographies.

Details on the availability of these publications may be obtained from:

SCIENTIFIC AND TECHNICAL INFORMATION DIVISION

NATIONAL AERONAUTICS AND SPACE ADMINISTRATION

Washington, D.C. 20546